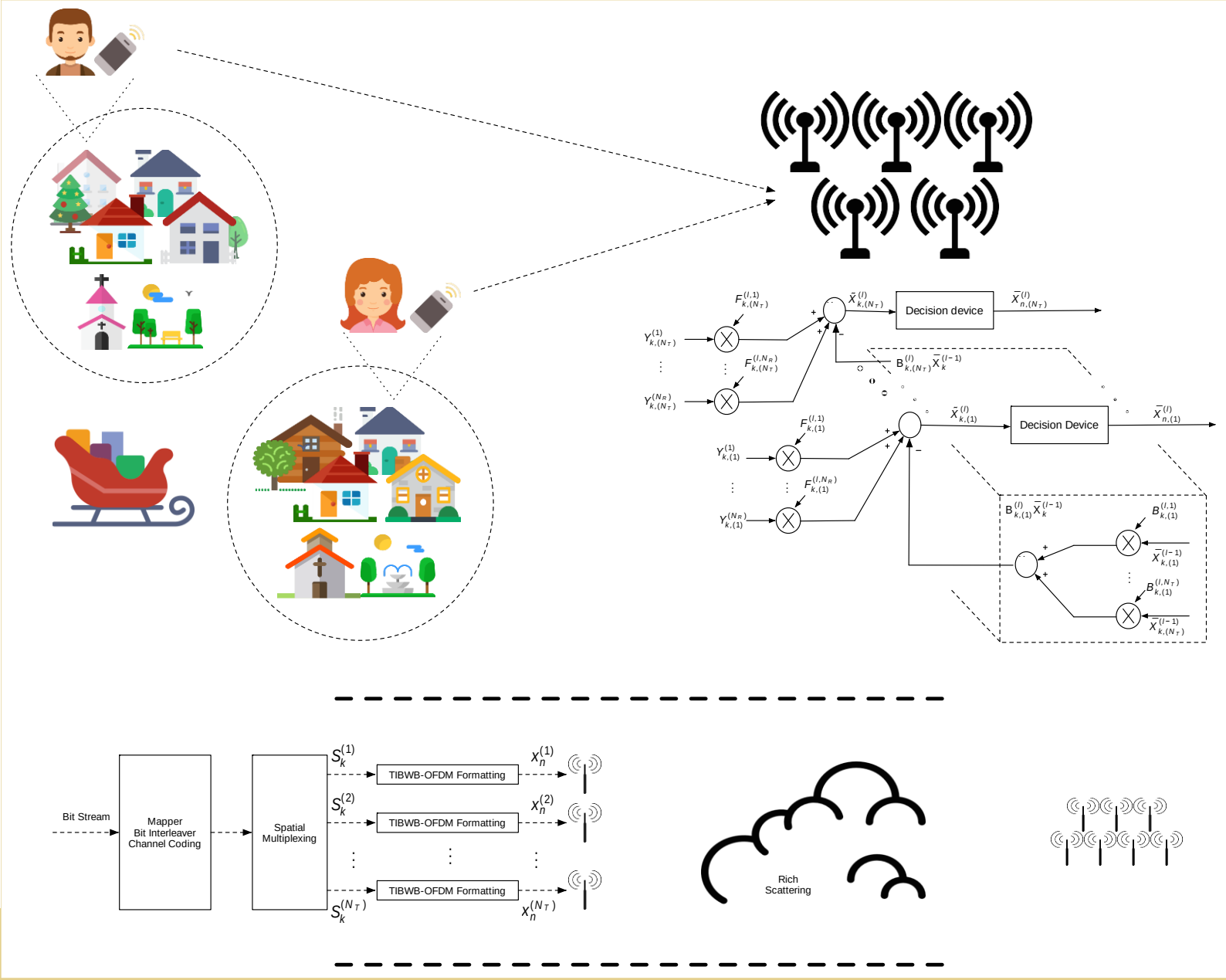

Andreia Pereira da Silva

Low Complexity Iterative Frequency Domain Equalisation for MIMO-OFDM Type Systems

Dissertação submetida para a satisfação parcial dos requisitos do grau de mestre em Engenharia Electrotécnica e de Computadores na especialidade de Telecomunicações

Dezembro, 2016

· U C ·

Universidade de Coimbra

FCTUC FACULDADE DE CIÊNCIAS
E TECNOLOGIA
UNIVERSIDADE DE COIMBRA

Low Complexity Iterative Frequency Domain Equalisation for MIMO-OFDM Type Systems

Andreia Pereira da Silva

Coimbra, December of 2016

Low Complexity Iterative Frequency Domain Equalisation for MIMO-OFDM Type Systems

Supervisor:

Prof. Dr. Marco Alexandre Cravo Gomes

Prof Dr. Vitor Silva

Jury:

Prof. Dra. Maria do Carmo Raposo de Medeiros

Prof. Dr. Marco Alexandre Cravo Gomes

Prof. Dra. Lúcia Maria dos Reis Albuquerque Martins

Dissertation submitted in partial fulfillment for the degree of Master of Science in Electrical and Computer Engineering.

Coimbra, December of 2016

Acknowledgements

Gostaria de começar por agradecer ao Professor Marco Gomes pela oportunidade de participar neste projeto, motivação, a ajuda nas várias dúvidas que surgiram no seguimento da dissertação e pela confiança que depositou em mim. Ao Professor Vitor Silva pela disponibilidade constante e pela sua capacidade de resolução de problemas. Ao Pedro Bento pela paciência inacabável e pelo tempo que perdeu comigo tanto no esclarecimento de conceitos teóricos como na componente prática e que claramente eu ganhei. Ao Professor Rui Dinis, que permitiu a minha participação nos seus projetos, pelo apoio e pela disponibilidade para tirar qualquer dúvida.

Ao Instituto de Telecomunicações que me acolheu e onde nunca faltou boa disposição por parte de todos os colegas e professores. À Fundação para a Ciência e Tecnologia pelo financiamento deste trabalho.

Aos meus pais, por quem sinto uma enorme gratidão e carinho sendo sempre totalmente apoiada em todos os meus projetos quer curricular ou extracurriculares. Ao meu irmão Diogo que mesmo estando longe ocupa e sempre ocupará uma grande parte do meu coração. Ao meu cão que me faz feliz todos os dias e por quem sinto um enorme afecto e carinho ocupando um lugar muito especial na minha família.

Aos meus amigos Ricardo Loureiro e ao César Martins pela boa disposição, por toda a ajuda oferecida e pela companhia durante as noitadas de trabalho.

Ao meu grupo de amigos, os "Zeros à Esquerda", os meus "Quiriiis", por todas as experiências vividas, por todas as noites bem passadas, pelo companheirismo e por todos os seus "avacalhanços".

Ao Pedro Apóstolo por todo o apoio que me deu durante o meu percurso académico, por todos os desabafos que teve de ouvir, ocupando um lugar muito importante na minha vida.

E finalmente à pessoa que devo parte daquilo que sou hoje, ao meu Querido Pedro Maça, que me apoia incondicionalmente em tudo, que me motiva todos os dias para ser uma pessoa melhor, que me ensina parte daquilo que é o mundo real e que virá a ser muito útil daqui para a frente, que tem toda a paciência de mundo para me ouvir e que me completa a todos os níveis.

Abstract

Wireless communications are, by any measure, the fastest growing segment of the communications industry. Not only the cellular phones, which have become a critical business tool and part of everyday life worldwide, but also computers and other data consuming devices have experienced exponential growth over the last decade, bringing some new challenges to the next generation wireless systems. Fifth generation wireless networks as the next standard must be able to meet the requirements imposed by the ever increasing demand in capacity, while guaranteeing robustness, reliability and higher data rates.

One of the most promising alternatives is the increase in the number of antennas in both transmitter and receiver, i.e. multiple-input multiple-output (MIMO) systems, which leveraged on signal processing techniques exploring added diversity may allow for higher spectral efficiency or improved robustness transmission. Regarding to achieve higher data rates and an increased capacity, employing spatial multiplexing combined with orthogonal frequency division multiplexing (OFDM) type systems is seen as one of most potential solutions. Particularly, when new techniques, such as the time-interleaved block-windowed burst OFDM (TIBWB-OFDM), are adopted is possible to achieve a highly spectral and power efficient wireless communication system, robust to the deep fades of the selective-frequency channel.

However, there is some computational complexity inherent to the MIMO systems, that grows with the number of antennas elements, making the receiver much more complex, namely the equalisation stage where state-of-the art equalisers, such as minimum mean squared error (MMSE) and zero forcing (ZF), require for the inversion of the channel's high dimension matrix. To overcome this problem, it is crucial to consider low complexity frequency-domain iterative receivers, such as equal gain combiner (EGC) and maximum ratio combiner (MRC), which do not require high dimension channel matrices inversions and as so, the receiver can be kept at an affordable complexity.

Therefore, the main goal of this work is to achieve a spectral and power efficient system able to handle with the impairments of the frequency-selective MIMO channel, while keeping the receiver complexity reduced through the use of techniques that does not require channel matrix inversions. Performance results shown that employing linear equalisers or nonlinear equalisers, such as EGC and MRC, allows substantial gains over the conventional MIMO employing cyclic prefix technique, in the same conditions. Furthermore, low complexity iterative methods have their best performances when employed in the multiple-input multiple-output TIBWB-OFDM (MIMO TIBWB-OFDM) scheme, achieving excellent performance and approaching the matched filter bound (MFB) with just a few iterations.

Keywords: MIMO-OFDM, OFDM, time-interleaved block-windowed burst OFDM, spatial multiplexing, maximum ratio combiner, equal gain combiner, minimum mean squared error.

Resumo

As comunicações sem fios são, sem sombra de dúvida, o segmento de mais rápido crescimento da indústria de comunicações. Não só os telemóveis, que se tornaram uma ferramenta fulcral no mundo dos negócios e parte da vida quotidiana em todo o mundo, mas também os computadores e outros dispositivos de consumo de dados têm vindo a experienciar um crescimento exponencial na última década, trazendo novos desafios para a próxima geração de sistemas sem fios. As redes sem fio de quinta geração como próximo standard deverão ser capazes de satisfazer os requisitos impostos pela crescente procura de maior capacidade, ao mesmo tempo que garantem robustez, fiabilidade e maiores taxas de transferência.

Uma das alternativas mais promissoras consiste no aumento do número de antenas tanto no transmissor como no recetor, isto é sistemas MIMO, que beneficiam de técnicas de processamento de sinal explorando uma diversidade adicional permitindo uma maior eficiência espectral ou uma transmissão robusta. No que diz respeito à obtenção de taxas de transferência de dados maiores e uma capacidade aumentada, empregando multiplexagem espacial combinada com sistemas OFDM ou que derivem dos mesmos é vista como uma das soluções mais poderosas. Particularmente, quando novas técnicas, como o TIBWB-OFDM, são adotados é possível obter um sistema de comunicação sem fios com uma melhor eficiência espectral e energética, robusto aos desvanecimentos profundos do canal selectivo na frequência.

No entanto, existe alguma complexidade computacional inerente aos sistemas MIMO, que aumenta com o número de antenas no sistema, tornando o recetor muito mais complexo, nomeadamente na fase de equalização onde equalizadores presentes no estado de arte, como o MMSE e ZF, necessitam de inversões de matrizes de altas dimensões. Para superar este problema, é crucial considerar recetores iterativos, tais como EGC e MRC, que não requerem inversões de matrizes de canal de altas dimensões e, como tal, o recetor pode ser mantido a uma complexidade razoável.

Portanto, o objetivo principal deste trabalho é conseguir um sistema com alta eficiência tanto a nível espectral como a nível energético, capaz de lidar com as deficiências do canal MIMO, enquanto a complexidade do recetor se mantém reduzida através do uso de técnicas que não necessitem de inverter as matrizes de canal. Os resultados obtidos mostraram que empregar equalizadores lineares ou não lineares, tais como o EGC and MRC, permite ganhos substanciais relativamente ao sistema conventional MIMO usando o prefixo cíclico como intervalo de guarda nas mesmas condições. Além disso, os métodos iterativos de baixa complexidade mostraram um melhor desempenho quando usados em esquemas do tipo MIMO TIBWB-OFDM, sendo conseguido um desempenho excelente capaz de aproximar o *match filter bound* com apenas algumas iterações.

Palavras Chave: MIMO-OFDM, OFDM, *time-interleaved block-windowed burst OFDM*, multiplexagem espacial, *maximum ratio combiner*, *equal gain combiner*, *minimum mean squared error*.

"Sometimes things fall apart so that better things can fall together"

— Marilyn Monroe

"One advantage of talking to yourself is that you know at least somebody's listening."

— Franklin P.Jones

"A dog is the only thing on earth that loves you more than he loves himself."

— Josh Billings

Contents

List of Acronyms

OFDM	orthogonal frequency division multiplexing
FDM	frequency division multiplexing
DAB	digital audio systems
DVB-T	terrestrial digital video systems
DVB-H	handheld digital video systems
ADSL	asymmetric digital subscriber line
VDSL	very high speed digital subscriber line
WLAN	wireless local area network
IFFT	inverse fast fourier transform
FFT	fast fourier transform
DFT	discrete fourier transform
IDFT	inverse discrete fourier transform
ICI	inter-carrier interference
ISI	inter-symbol interference
PAPR	peak-to-average power ratio
OOB	out-of-band
CP	cyclic prefix
ZP	zero padding
CS	cyclic suffix
SRRC	square-root raised cosine
CP-OFDM	cyclic-prefixed OFDM
ZP-OFDM	zero-padding OFDM

BWB-OFDM block-windowed burst OFDM

TIBWB-OFDM time-interleaved block-windowed burst OFDM

PSD power spectral density

FEC forward error correction

SNR signal-to-noise ratio

SC-FDE single carrier-frequency domain equalisation

BER bit error rate

SC single carrier

AWGN additive white gaussian noise

FDE frequency domain equalisation

ZF zero forcing

MMSE minimum mean squared error

MIMO multiple-input multiple-output

MISO multiple-input single-output

SIMO single-input multiple-output

SISO single-input single-output

SISO CP-OFDM single-input single-output CP-OFDM

MIMO-OFDM multiple-input multiple-output OFDM

MIMO CP-OFDM multiple-input multiple-output CP-OFDM

MIMO TIBWB-OFDM multiple-input multiple-output TIBWB-OFDM

MIMO BWB-OFDM multiple-input multiple-output BWB-OFDM

MU-MIMO multi-user MIMO

SU-MIMO single-user MIMO

SM spatial multiplexing

SD spatial diversity

ACI adjacent channel interference

EGC equal gain combiner

MRC	maximum ratio combiner
DFE	domain frequency equalisation
BS	base station
QPSK	quadrature phase shift keying
MFB	matched filter bound
IB-DFE	iterative-block frequency domain equalisation
LDPC	low-density parity-check
LLR	log-likelihood ratio

List of Figures

1 Introduction

The growth of smartphones, tablets, laptops, and many other wireless data consuming devices, brings some challenges to the next generation wireless systems in order to support a high quality service. Hence, robustness, reliability and higher data rates are key factors for the future wireless communication systems [16]. The emergence of multiple-input multiple-output (MIMO) technologies constitutes one of the most significant breakthroughs in the design of wireless communication systems, being already adopted by many wireless standards [4]. The use of multiple antennas at the transmitter and receiver delivers significant performance improvements, namely in data transmission and transmission reliability [4], over the conventional single-input single-output (SISO) systems. Thus, two different approaches can be considered in MIMO technique: either the enhancement of the system reliability through the spatial diversity [13] or the increase of the data transmission rate through spatial multiplexing [29], being possible to achieve both gains simultaneously by assuring a tradeoff between them [27]. Therefore, MIMO is a crucial technique able to face the impairments of the wireless channel as well as the strict power and bandwidth constraints, concerning a robust transmission, small transmit powers and high spectral efficiencies.

On the other hand, orthogonal frequency division multiplexing (OFDM) has become a popular multi-carrier modulation technique for wireless communication systems [9]. In fact, OFDM turns the frequency-selective channel into a set of parallel, overlapped and orthogonal narrow band flat fading sub-channels, achieving a significant spectral efficiency in comparison with conventional frequency division multiplexing (FDM) multicarrier transmission systems, and avoiding possible inter-carrier interference (ICI) by the orthogonality condition. Other basic principle that underlies OFDM is the insertion of a guard interval, called cyclic prefix (CP), which is a copy of the last part of the OFDM symbol, used to accommodate the dispersive channel effect and therefore mitigate the usual inter-symbol interference (ISI) [10]. Furthermore, since the overall frequency-selective channel is converted into a set of parallel flat fading channels, the equalisation task is drastically simplified, enabling a low computational complexity [33]. However, OFDM comes with several drawbacks that motivates an emergence of alternative schemes, namely its high out-of-band (OOB), high peak-to-average power ratio (PAPR) and a loss in spectral and power efficiency owing to the use of CP. For this reason, the block-windowed burst OFDM (BWB-OFDM) transceiver scheme was proposed in [26] [33]. This scheme aims to reach a commitment between higher transmission rate and better spectrum confinement, while maintaining the orthogonality between subcarriers that allows for a simple equalisation. The reason for such improvements is the use of a zero padding (ZP) guard interval and the employment of a smoother and non-rectangular window, such as the square-root raised cosine (SRRC) window, providing a superior power and spectral efficiency. Nevertheless, performances based on both OFDM and BWB-OFDM transmission techniques can be adversely affected by the deep fades of the time-dispersive channel. For this

reason, the recent TIBWB-OFDM transceiver was proposed in [38] [41], allowing to reduce significantly the damage caused by those deep fading occurrences through the replication of the information throughout the assigned bandwidth, preserving the same advantages of the BWB-OFDM scheme.

By combining MIMO employing spatial multiplexing (SM) and those OFDM type techniques, an enhanced high speed wireless communication system is attained, enjoying both benefits from both technologies. Particularly, when time-interleaved block-windowed burst OFDM (TIBWB-OFDM) is the assumed scheme, a new highly spectral and power efficient wireless communication system emerges, denoted as MIMO TIBWB-OFDM, able to handle the impairments of the frequency selective MIMO channel.

1.1 Motivation and Objectives

Even though it is possible to achieve a highly spectral and power efficient system able to deal with the deep fades of the time-dispersive channel, it is crucial to maintain the receiver simplicity reduced, since its complexity increases enormously with the number of transmit and receive antennas. Thus, there is in need the employment of low complexity equalisers, such as equal gain combiner (EGC) [22] and maximum ratio combiner (MRC) [22], that do not require channel matrix inversions as state-of-the art traditional linear equalisers, such as minimum mean squared error (MMSE) and the zero-forcing (ZF) equalisers, and able to approach the matched filter bound (MFB). Consequently, the channel effects are not completely removed, having a high ISI effect associated besides the interference between transmitted streams. Hence, iterative frequency domain equalisers based on EGC and MRC [2] [6] [14] are desired, being also called as nonlinear equalisers, in order to cancel the high residual interference levels.

As so, the goal of this thesis is to develop a MIMO system built on the TIBWB-OFDM technique with high spectral and power efficiency and to evaluate the benefits of the employment of both iterative EGC and MRC equalisers in both multiple-input multiple-output OFDM (MIMO-OFDM) and MIMO TIBWB-OFDM schemes, aiming to achieve systems with reduced complexity and performances as close to MFB as possible.

1.2 Dissertation Outline

This first chapter provides a brief overview of the topic in order to justify and motivate the analyses developed in the thesis. The remaining contents of the dissertation are divided into more six chapters, organised in the following way:

Chapter 2

This chapter introduces the concept of OFDM as well as some of its advantages and disadvantages, with a brief system analysis. It is also presented the BWB-OFDM approach, an improved version of the conventional cyclic-prefixed OFDM (CP-OFDM) scheme, describing its architecture and its overall improvements. Later in this chapter, the TIBWB-OFDM scheme is introduced, where the theoretical aspects and the architecture behind it are discussed, emphasising the overall improvements towards the BWB-OFDM scheme. Finally, these three techniques are compared employing a MMSE equaliser.

Chapter 3

This chapter introduces the MIMO technique, focusing on its system model and its techniques, such as spatial diversity (SD) and SM, that provides the diversity gain and multiplexing gain, respectively, or the combination of both to the system.

Chapter 4

On this chapter, the conventional MIMO-OFDM is presented, exposing its system model and its advantages and disadvantages. Moreover, several equalisation techniques (including linear and nonlinear) employed in MIMO-OFDM, such as MMSE and the iterative EGC and MRC, will also be discussed in detail.

Chapter 5

This chapter describes the architecture of the developed MIMO TIBWB-OFDM scheme.

Chapter 6

This chapter presents the performance results of three scenarios using different types of receivers considering both coded and uncoded transmissions. Firstly, an analysis over the multiple-input multiple-output CP-OFDM (MIMO CP-OFDM) is taken into account, being the performance of the conventional single-input single-output CP-OFDM (SISO CP-OFDM) and MIMO CP-OFDM techniques compared employing the ZP and MMSE equalisers, in order to analyse the gains achieved when a MIMO system is regarded. In addition, it is also presented a comparison between the iterative MRC and EGC and the linear MMSE receivers. Finally, the discussion of the MIMO TIBWB-OFDM technique is considered, being compared with the conventional MIMO CP-OFDM to confirm the superior performance over the latter. Then, the MIMO TIBWB-OFDM scheme performances employing the iterative MRC and EGC and the linear MMSE receivers are compared and analysed. In order to certify that the MIMO TIBWB-OFDM scheme has an improvement towards multiple-input multiple-output BWB-OFDM (MIMO BWB-OFDM) scheme, their performances employing the previously mentioned receivers are also presented.

Chapter 7

This chapter concludes and summarises the results of this thesis and presents some future research lines.

2 Multicarrier Communication Systems

Multicarrier modulation is currently used in many broadband wireless multimedia communication systems due to its robustness against the radio channel impairments, namely frequency-selective fading, enabling to deal with ICI and ISI. The frequency selective channel affects the transmitted signal by attenuating not in the same way its different frequency components and, therefore, experiencing different levels of fading.

The basic idea of multicarrier modulation is to separate a high rate data stream into several low-rate data sub-streams, each one modulating a different subcarrier. Because of the available bandwidth is being divided into thin slices per each parallel transmitted signal, the aforementioned characteristic guarantees that within each sub-band fading attenuation can be considered constant, empowering simple equalisation. However, in severe time-dispersive environments, the use of error correcting codes may still be crucial to handle with strong deep fading occurrences [9].

OFDM [31] is possibly the most widely used form of multicarrier modulation, because of its promising spectral efficiency when compared with the conventional FDM multicarrier transmission systems. While in the latter, the frequency band is divided into a few non-overlapping frequency subchannels in order to avoid the possible adjacent channel interference (ACI), in OFDM all the frequency subchannels are overlapped because of its orthogonality, saving a substantial amount of spectrum. However, it has also some drawbacks, like the high PAPR of the OFDM signal that decreases the system power efficiency [37] and the need to use a long CP, in order to deal with channel time-dispersion that also considerably decreases the power efficiency and decreases the throughput. In this regard, new multicarrier techniques have been proposed, such as Block-Windowed Burst OFDM [26] [33] that is discussed later in this chapter.

Another problem that is common to OFDM and BWB-OFDM technique is the deep fades of the time-dispersive channel, whose effect on a transmission scheme could be devastating, being, inside a deep fading region, a given spectral content completely destroyed. In this way, an improved version of BWB-OFDM, entitled Time-Interleaved BWB-OFDM [38] [41], has been developed and will be described in this chapter as well.

2.1 OFDM

OFDM is a multicarrier modulation technique [9], where a single stream is transmitted by a given number of subcarriers, which are orthogonal with each other. One of the main advantages of OFDM is the use of the inverse fast fourier transform (IFFT) and fast fourier transform (FFT) processes in order to reach an efficient implementation of the resulting orthogonal signals. Furthermore, OFDM empowers the separation of high-rate data stream into a given number of low-rate sub-streams transmitted in parallel over

different overlapping frequency bands, providing bandwidth efficiency [33] and avoiding ICI guaranteed by the orthogonality between the subcarriers [9] as shown in Figure 2.1. As a result, the transmitted signals are also orthogonal and independent with each other, enabling its detection without any interference.

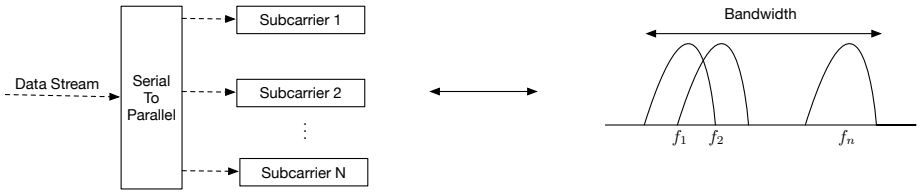

Figure 2.1: Bandwidth used in OFDM systems, whose subcarriers are overlapped in the frequency domain.

OFDM is a very popular technique, widely used in many of the latest wireless and telecommunications standards [18] [36] [39], namely for digital broadcasting systems (digital audio systems (DAB), terrestrial digital video systems (DVB-T) and handheld digital video systems (DVB-H)), home networking (asymmetric digital subscriber line (ADSL) and very high speed digital subscriber line (VDSL)), wireless local area network (WLAN) standards (HyperLAN/2 and IEEE 802.11 a/g/j/n), etc.

2.1.1 Representation of the OFDM Signal and Orthogonality

Referring to Figure 2.1, consider that the original bit stream is mapped into complex symbols of a M-ary constellation χ with T_s being the the symbol duration at the output of the modulator. Assume an OFDM signal with N sub-carriers and denote $X_{k,l}$:{k=0,1,...,$N-1$} as the l^{th} transmitted OFDM symbol in the interval $lT_{sym} \leq t < (l+1)T_{sym}$ with $T_{sym} = NT_s$ that results from splitting the original data stream into N sub-streams having rate $1/NT_s$, and let $f_k = k/T_{sym}$ be the k^{th} carrier frequency of X_k. The baseband modulated OFDM signal in the continuous domain can thus be written as

$$x_l(t) = \sum_{k=0}^{N-1} X_{k,l} e^{j2\pi f_k t} \quad , \quad lT_{sym} \leq t < (l-1)T_{sym} \quad . \tag{2.1}$$

For easy of understanding and without loss of generalisation, from now on it will be considered that $l = 0$. The correspondent OFDM signal in the discrete time is obtained by sampling it at rate $f_s = 1/T_s$, i.e. by making $t = nT_s$, and is expressed by:

$$x_n = x(nT_s) = \sum_{k=0}^{N-1} X_k e^{j2\pi n \frac{k}{N}} \quad , \tag{2.2}$$

which can be recognised as the inverse discrete fourier transform (IDFT) that can be efficiently computed using the IFFT when N is a power of 2 [23]. The minimum frequency spacing between the subcarriers in order to have the orthogonality condition satisfied is $\Delta f = 1/NT_s$. Hence, $f_k = k\Delta f = k/NT_s$, with $k = 0, 1, .., N-1$. In the digital domain, the orthogonality condition can be easily proved by computing [10]:

$$\frac{1}{N} \sum_{k=0}^{N-1} e^{j2\pi k \frac{n}{N}} e^{-j2\pi i \frac{n}{N}} dt = \frac{1}{N} \sum_{k=0}^{N-1} e^{j2\pi (k-i) \frac{n}{N}} dt = \begin{cases} 1 & k = i \\ 0 & k \neq i \end{cases} \quad , \tag{2.3}$$

with both $e^{2\pi k \frac{n}{N}}$ and $e^{2\pi i \frac{n}{N}}$ representing two different subcarriers exponentials.

2.1.2 Guard Interval

When the channel introduces time dispersion, due to multipath propagation, and the delay spread is larger than the symbol period, frequency selective fading arises [9]. Unfortunately, it is not easy to compensate this, since its characteristics are random and impossible to be predicted. However, one of the many advantages of OFDM is its ability to deal with the multipath fading, namely by splitting the incoming data into N subcarriers increasing the symbol time N times, which reduces the weight of the multipath delay spread relative to the symbol time by the same factor [25] and, also the possibility of appending a guard interval time for each OFDM symbol [10] .

If the introduction of the guard interval is chosen to be larger than the expected delay spread of the wireless channel, not only is the ISI almost completely eliminated but the ICI can be prevented by choosing the right type of guard interval. It can be performed by three types, such as ZP, CP and cyclic suffix (CS) [10].

Cyclic Prefix

The CP, represented by a copy of the last samples of each OFDM symbol, is attached in the beginning of the mentioned symbol [30]. Its insertion provides periodicity to the symbol, which simplifies the reception of the signal based on the FFT technique, as well as orthogonality between subcarriers, by ensuring that there will be always a complete symbol within the FFT window. This allows in an easy way to mitigate the effect of ISI by keeping the orthogonality and solves the problem of ICI.

Although CP-OFDM has some important advantages, it comes with a decrease of the overall data rate by $T/T'_{sym} = T_{sym}/(T_{sym}+T_{cp})$ and a power efficiency loss as well since a part of the signal energy is wasted in transmitting the CP. To overcome the latter problem, an alternative consists in taking a ZP approach.

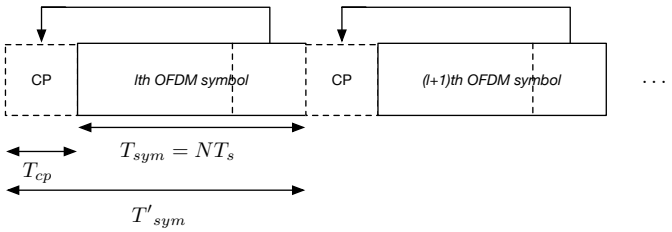

Figure 2.2: OFDM symbols with CP insertion.

Zero Padding

This solution appends zero samples to the OFDM symbol, in other words, it replaces the time domain redundancy of CP approach by null samples. If the subcarriers don't suffer from the same delay, the performance of zero-padding OFDM (ZP-OFDM) will be compromised, with the orthogonality between them being destroyed and ICI effect arising, since the product 2.3 will no longer be zero, which complicates the receiver design.

So, although in comparison with CP approach, ZP-OFDM has lower transmission power for the same OFDM symbol length and a simpler transmitter scheme, no longer the easy equalisation promoted by the

CP is possible. Hence, the CP approach continues being regarded as the best choice when compared with the others.

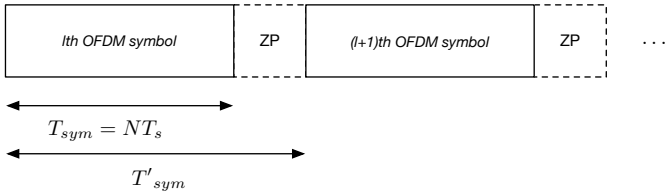

Figure 2.3: OFDM symbols with ZP insertion.

2.1.3 Other Issues

The combination of several signals of different subcarriers makes OFDM suffers from transmission power level fluctuation with the OFDM signal having an high PAPR. This requires the use of a linear power amplifier at the transmitter front-end and its operation at a quite inefficient operating point in terms of power consumption, i.e. with a large amount of back-off, in order to avoid amplifier saturation [24] and signal non-linear distortion (and hence, mitigate the possible loss of orthogonality between subcarriers and spectral spreading). In addition to this poor efficiency, linear power amplifiers with a high dynamic range are too expensive.

OFDM is also highly sensible to time and frequency synchronisation errors and, especially in the last case where it can experience a high bit error rate (BER). This happens not only because of the relative movement between transmitter and receiver, but also because of the difference between local oscillator frequencies in transmitter and receiver. All mentioned previously result in a loss of orthogonality, lowering the overall performance of the system.

Finally, another disadvantage of OFDM is the high OOB radiation since its spectrum is the sum of many frequency-shifted sinc functions, which have a large OOB power. For this reason, it is necessary to have a better spectrum confinement, which can be improved using windowing methods [42], as it will be discussed in the next section.

2.2 Block-Windowed Burst OFDM

As mentioned previously, OFDM has been widely adopted in many standards, becoming a very appealing and promising multicarrier technique. The reason for such success is due to its convenient advantages, such as bandwidth efficiency, low complexity of the FFT-based transceiver, above average BER performance and robustness against frequency selective fading [31]. OFDM drawbacks such as a high PAPR and considerable OOB radiation have tried to be improved during OFDM lifespan, with the proposal of several PAPR reduction techniques (e.g. tone reservation, selective mapping, partial transmitted sequence) [37] and filtered OFDM techniques [17] in order to enhance spectral efficiency and reduce OOB radiation. While some of the OFDM advantages come from the use of a CP, this also brings constrains: the reduction of overall data rate and the decrease of the power efficiency, given the power waste on transmission of the CP whose length can reach up to 25% of the OFDM symbol length [10]. To tackle these problems jointly with the fact that the

OFDM scheme has its spectrum with a high level of the sidelobes, and thereby suffering from high OOB radiation, a new transceiver entitled Block-Windowed Burst OFDM was proposed in [26] [33].

The BWB-OFDM technique packs together several windowed OFDM based blocks, with a sole ZP added at the end. This approach represents a hybrid block transmission technique, where in the transmitter side it is employed a typical windowed OFDM tecnique, while in the receiver side the signal is seen as of a single carrier (SC)-type and single carrier-frequency domain equalisation (SC-FDE) is used, allowing to achieve higher both spectral and power efficiency. In fact, leveraging on a time-domain SRRC window profile, this scheme can reach either a better spectrum confinement maintaining the same data rate that CP-OFDM provides or higher data rate maintaining the spectrum of the CP-OFDM scheme [26]. This use of a SRRC filter at both transmitter and receiver, providing better matching characteristics and thereby mitigating the ICI effect and improving the overall signal-to-noise ratio (SNR) by reducing the level of the spectrum sidelobes.

In [26] and [33] it is shown that BWB-OFDM transceiver enables:

- Transmission rates up to 11% higher that typical OFDM scheme, by keeping the same transmission rate as OFDM;
- Gains ranging from 35 to 45dB in spectral confinement, reckoning on the window's roll-off.

2.2.1 Transmitter

The new designed BWB-OFDM transmitter is built on the filtered OFDM scheme [33], whose main intention is to achieve a power spectral density (PSD) with lower OOB radiation, and improve the power efficiency by reducing the need for a CP per each OFDM block. In Figure 2.4 is presented the BWB-OFDM transmitter.

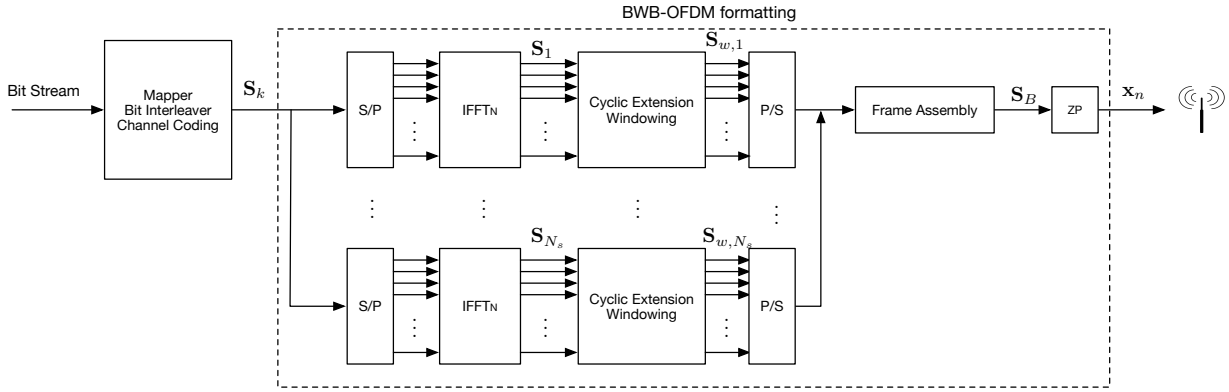

Figure 2.4: BWB-OFDM Transmitter Scheme [26].

As mentioned previously, a typical OFDM scheme is applied in the transmitter side, in which the input bit stream is mapped into a given M-ary constellation, with the obtained symbols being assign to different carriers. Modulation mapping can be preceded by channel decoding and interleaving, that are known to be key techniques for improving the BER performance of OFDM techniques in severe time-dispersive channels. By using IFFT process, those modulated symbols are divided into N narrow-band, low rate, frequency non-selective substreams and transmitted in parallel.

Let S_k:{k=0,1,...,$N-1$} be the modulated symbol at the k^{th} subcarrier. In the discrete time domain, the complex envelope of baseband conventional OFDM symbol given by (2.2), can be written as,

$$s_n = \sum_{k=0}^{N-1} S_k w[n] e^{j2\pi k \frac{n}{N}} \quad , \quad n = 0, 1, ..N-1 \tag{2.4}$$

where $w[n]$ is a unitary rectangular pulse with length N. The subcarriers are kept orthogonal with each other, being frequency spaced of $1/N$.

The BWB-OFDM scheme employs instead a smoother (non-rectangular) window, typically a SRRC window, aiming to decrease the OFDM's high spectrum sidelobes and thereby a full cancellation of ICI. Figure 2.5 shows the considerable gains reached in spectrum confinement by the use of SRRC windows with different roll-offs, whose expression for a given roll-off β is,

$$h_{SRRC}[n] = \begin{cases} 1 & |n| \leq \frac{N}{2}(1-\beta) \\ \cos\left(\frac{\pi}{4\beta}\left[\frac{2n}{N} - (1-\beta)\right]\right) & \frac{N}{2}(1-\beta) \leq |n| \leq \frac{N}{2}(1+\beta) \\ 0 & |n| \geq \frac{N}{2}(1+\beta) \end{cases} , \tag{2.5}$$

where $n = -N, ..., N$.

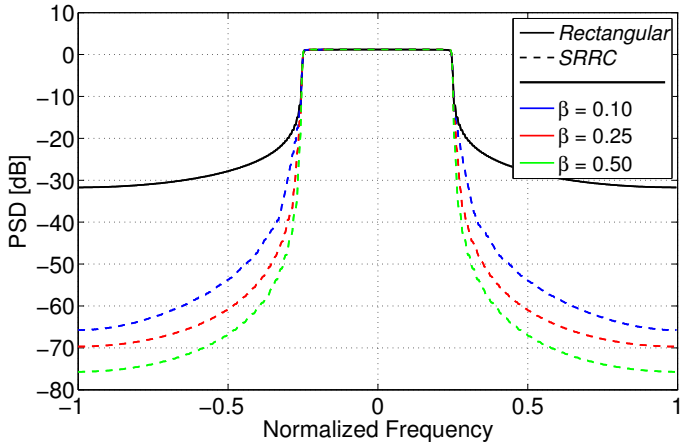

Figure 2.5: PSD of the transmitted signal applying a SRRC window [26].

Compared with filtered OFDM, whose spectrum confinement is achieved through conventional filtering techniques [8], BWB-OFDM has less control over spectrum confinement, being more convenient in sense of complexity, since the windowing process requires just a few multiplications over the samples that fall into the roll-off region. This reduction of complexity can go far as one order of magnitude [31]. As a result, the windowed symbol is represented by,

$$\mathbf{s}_w = [\quad \mathbf{s}_n \quad | \quad \mathbf{s}_n \quad]_{(1\times 2N)} \quad \odot \quad \mathbf{h}_{SRRC(1\times 2N)} \quad , \tag{2.6}$$

where the operator $\odot$ is a point-wise product and bold lettering is used to denote a vector, i.e, $\mathbf{x}_{(1\times N)} = [x_0 ... x_{N-1}]$.

Although the improved spectrum confinement is achieved at the cost of an increased of the number of samples per transmitted symbol to $N(1+\beta)$ (bordering zeros resulting from the $\odot$ product are discarded),

the symbol energy remains the same, on the contrary of what is verified in a CP-OFDM system, which handles with an increase of the symbol energy and so that introduces a power penalty (i.e. a loss of the effective transmit power).

The N_s OFDM blocks (i.e a set of symbols $\mathbf{s}_{w,j}$ with $j = 1, ..., N_s$) are packed together and written as,

$$\mathbf{s}_B = [\quad \mathbf{s}_{w,1} \quad | \quad \mathbf{s}_{w,2} \quad | \quad ... \quad | \quad \mathbf{s}_{w,N_\mathbf{s}} \quad]_{(1\times N_B)} \quad , \tag{2.7}$$

having length $N_B = N_s \times N(1+\beta)$. In order to deal with time-dispersive channel's delay spread, a ZP interval guard is then inserted at the end of the block of N_s OFDM symbols, s_B, being obtained the BWB-OFDM symbol and given by,

$$\mathbf{x}_n = [\quad \mathbf{s}_B \quad | \quad \mathbf{0}_{(1\times N_{ZP})} \quad]_{(1\times N_x)} \quad , \tag{2.8}$$

where $\mathbf{0}_{1\times N_{ZP}}$ is a null vector representing the ZP guard interval with length N_{ZP}, and with final length of the BWB-OFDM symbol given by $N_x = N_s \times N(1+\beta) + N_{ZP}$.

2.2.2 Receiver

In Figure 2.6 is presented the BWB-OFDM receiver architecture. The received BWB-OFDM block when handled as a whole can be regarded as of sort of block-based SC transmission type [3], being possible to employ SC-FDE.

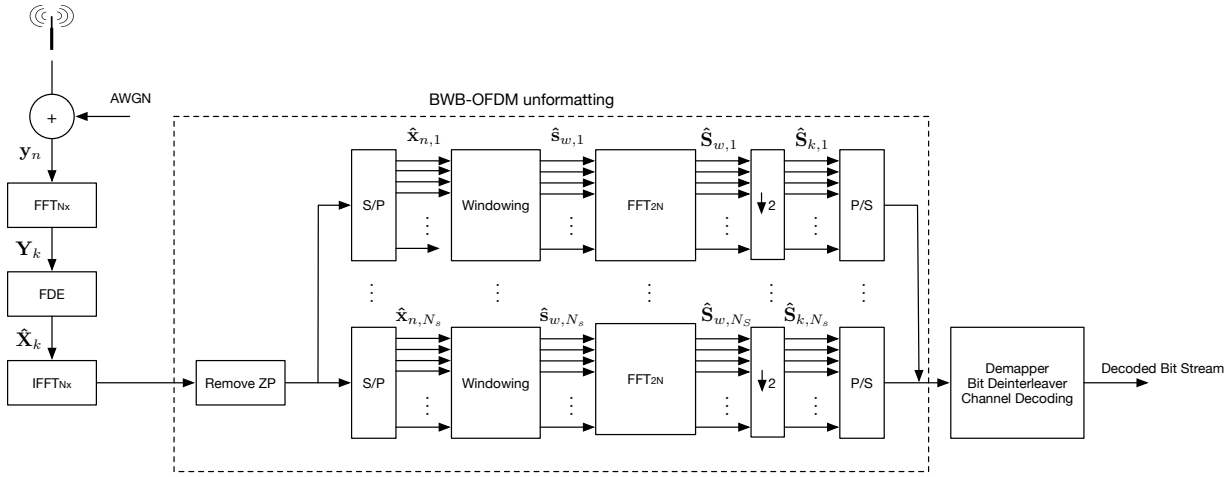

Figure 2.6: BWB-OFDM Receiver Scheme [26].

Firstly, the received time-domain BWB-OFDM block $\mathbf{y}_n$ of length N_x is converted to the frequency domain by applying FFT technique giving rise to Y_k. When N_{ZP} is longer than the delay spread of the channel, $\mathbf{Y}_k$ can be expressed as,

$$\mathbf{Y}_k = \mathbf{H}_k\mathbf{X}_k + \mathbf{N}_k \quad , \tag{2.9}$$

where $\mathbf{X}_k$ is the BWB-OFDM transmitted symbol in the frequency domain and $\mathbf{H}_k$ and $\mathbf{N}_k$ denote, at the k^{th} subcarrier, the channel frequency response and the complex additive white gaussian noise (AWGN), respectively.

Emphasis is then put on equalisation employing known frequency domain equalisation (FDE) techniques,

e.g. ZF [31], MMSE [28], iterative-block frequency domain equalisation (IB-DFE) [3] [11], or others.

After achieving the equalised signal $\hat{\mathbf{X}}_k$ and converting it to the time-domain by the means of a N_x-sized IFFT, the cyclic extension ZP is removed, giving rise to the megablock x_n with length $N_s \times N(1+\beta)$. Then, the megablock is separated into symbols $\hat{x}_{n,j}$, with $j = 1, ..., N_s$. An equal number of zeros is appended at both ends of each symbol $\hat{x}_{n,j}$, in order to increase its length up to $2N$, followed by applying the same windowing process performed in the transmitter (matched filtering), being represented by,

$$\hat{\mathbf{s}}_{w,j} \quad = \quad \hat{\mathbf{x}}_{n,j(1\times 2N)} \quad \odot \quad \mathbf{h}_{srrc(1\times 2N)} \tag{2.10}$$

The symbols given by (2.10) are converted to the frequency-domain by the means of a 2N-sized FFT and downsampled by 2, being the original data $\mathbf{S}_k$ of the j^{th} OFDM symbol estimated as,

$$\hat{\mathbf{S}}_{k,j}[m] \quad = \quad \hat{\mathbf{S}}_{w,j}[2m]_{(1\times 2N)} \quad , \quad m = 0, 1, ..N-1 \tag{2.11}$$

Finally, to get the original bit stream, on each $\hat{\mathbf{S}}_{k,j}$ it is applied the original bit deinterleaving and channel decoding.

2.3 Time-Interleaved BWB-OFDM

The transceiver scheme proposed in [26] [33] allows a commitment between signal spectrum confinement and higher transmission rate, while keeping the orthogonality between subcarriers that enables a simple FDE. In fact, since this approach does not use a CP guard interval per transmitted OFDM symbol, BWB-OFDM can achieve higher data rates by maintaining the same spectrum of the CP-OFDM scheme, or alternatively, more compact spectrum by maintaining the same data rate of CP-OFDM scheme. Moreover, the appending of the guard interval ZP per N_s OFDM symbols permits a considerable increase in terms of energy efficiency. The PAPR level is also decreased [1], not being mandatory to use power amplifiers with a high dynamic range. However, the system has some drawbacks when transmitting over hostile channel conditions, namely due to the deep fades associated to severe time-dispersive channels. Actually, the effects of those deep fades can be devastating, being possible to have all or part of the transmitted information completely destroyed.

The TIBWB-OFDM scheme proposed in [38] [41] represents an improved approach able to deal with the deep fades of the time-dispersive channel. More specifically, the original information is replicated throughout the assigned bandwidth in order to preserve all data susceptible of being destroyed.

Let's consider the original BWB-OFDM symbol and its j^{th} windowed-OFDM component block symbol $s_{w,j}$ with length $N(1+\beta)$, with $j = 1, ..., N_s$. By expanding each sequence $s_{w,j}$ individually by a N_s factor, its spectrum will present $N_s - 1$ compressed replicas of the original spectrum. The resulting expanded component base-blocks OFDM of the BWB-OFDM symbol can be written as,

$$s_{e,j} = \begin{cases} s_{w,j}\,[n/N_s] & \text{if n mod} \quad N_s = 0 \\ 0 & \text{if otherwise} \end{cases} \quad , \tag{2.12}$$

[1] The TIBWB-OFDM megablock and the OFDM block have the same length.

for $n = 0, 1, ..., N_B$ with $N_B = N_s \times N(\beta + 1)$. A somehow equivalent TIBWB-OFDM can be formed from the juxtaposition sum of expanded symbols $s_{e,j}[n]$, with unitary time delay between consecutive symbols, filling the zero gaps (i.e. zeros inserted through the expansion process) of each other.

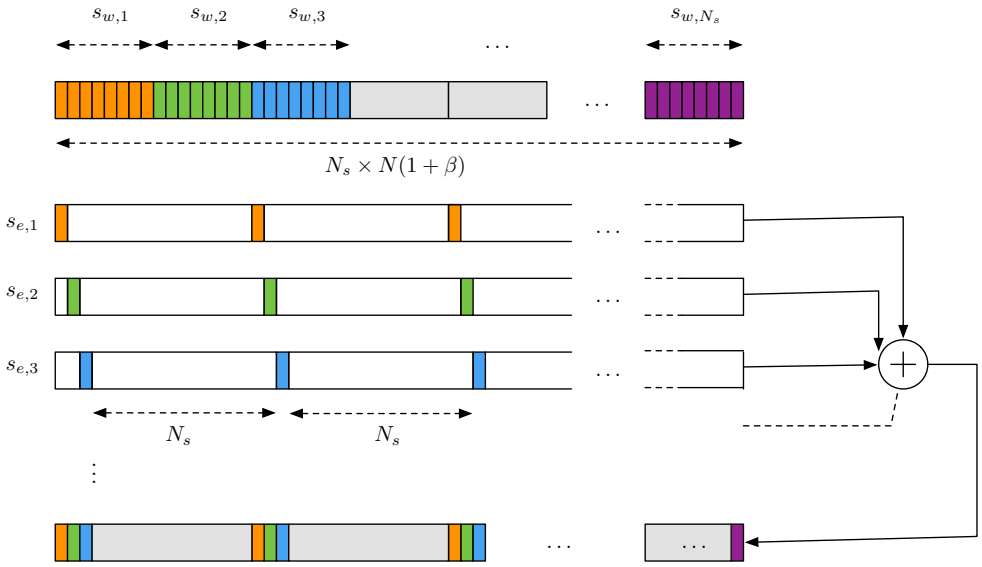

Figure 2.7: Time Interleaved BWB-OFDM transmitted block.

The resulting sequence can be expressed as,

$$s_{B\pi}[n] = \sum_{m=0}^{N_s-1} s_{e,j}[n-i] \quad , \tag{2.13}$$

being, therefore, this sequence result from a time-interleaving of the samples of the original BWB-OFDM symbol and, as so, the mentioned sequence $s_{B\pi}$ is denoted as Time-Interleaved BWB-OFDM symbol. The spectrum of (2.13) can be written as,

$$S_{B\pi}\left(e^{jw}\right) = \sum_{m=0}^{N_s-1} S_{e,j}\left(e^{jw}\right) e^{-jwm} \quad , \tag{2.14}$$

where $S_{e,j}(e^{jw}) = S_{w,j}(e^{jwN_s})$ is the spectrum of the j^{th} expanded windowed-OFDM component symbol. Since there is a time expansion, the spectra of each the symbols $s_{w,j}$ is replicated in the frequency N_s times, still having a superposition of the spectra of each of these individual symbols.

Note that, the overall bandwidth of the proposed TIBWB-OFDM symbol remains the same of the BWB-OFDM, because of the guarantee of the same time duration of both BWB-OFDM and TIBWB-OFDM and, therefore, the same sampling rate, given by the time-interleaving procedure. However, the spectrum of TIBWB-OFDM symbol can be seen (in a simplistic way) as a compressed spectrum of the BWB-OFDM symbol by a N_s factor, and replicate this one N_s times.

To conclude, when the channel has a deep fade region around a certain range of frequencies, the spectral content inside that region will be completely destroyed, being that information lost. Nevertheless, since the time-interleaving approach enables to replicate the data throughout the assigned bandwidth, it makes possible to recover part of it from the remaining unaffected regions that contain the same information.

2.3.1 Transmitter and Receiver

The proposed TIBWB-OFDM transmitter [38] [41] is built on the BWB-OFDM transmitter [26] [33], being presented in the Figure 2.8. This improved transceiver employs time-interleaving and windowing in order to perform spectral shaping. Consequently, the assembly process of the OFDM based symbols to construct the $\mathbf{s}_B$ is what differs from the BWB-OFDM transceiver.

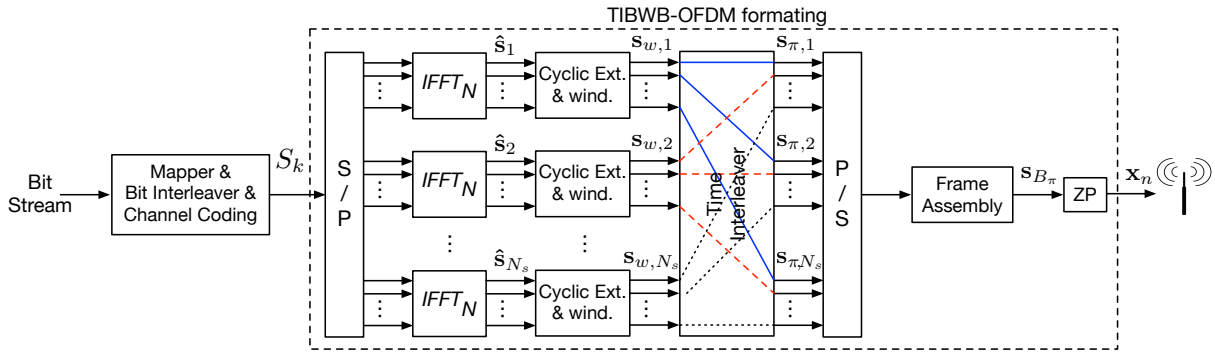

Figure 2.8: TIBWB-OFDM Transmitter Scheme [41].

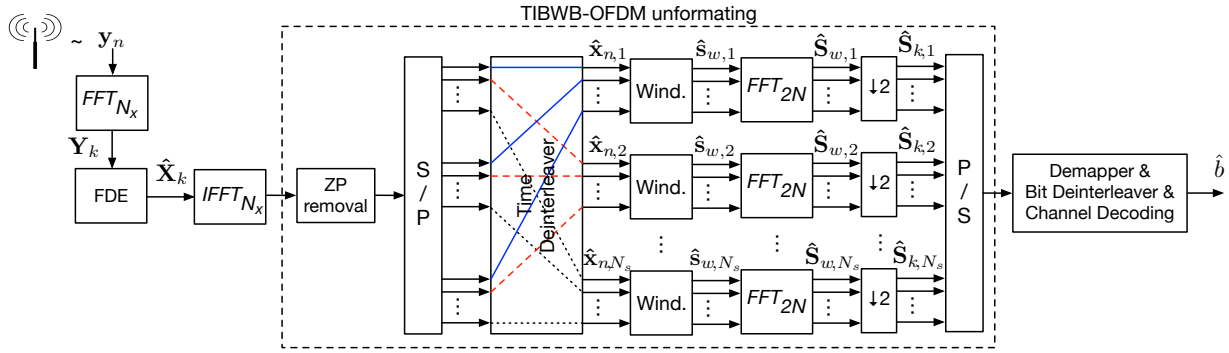

Figure 2.9: TIBWB-OFDM Receiver Scheme [41].

In this case, the time-interleaver is performed after the cyclic extension and windowing stage, where the resulting symbols $\mathbf{s}_{w,j}$, with $j = 1, ..., N_s$, are interleaved between each other, whose permutation matrix $\mathbf{\Pi}$ follow the procedure shown in the Figure 2.8, resulting in N_s interleaved symbols $\mathbf{s}_{\pi,j}$ and being given as,

$$\mathbf{s}_{B\pi} = \mathbf{\Pi}\mathbf{s}_B \quad , \tag{2.15}$$

where s_B can be written as (2.7) being the set of OFDM symbols $s_{w,j}$ packed together with $j = 1, ..., N_s$.

In other hand, at the receiver, the time-deinterleaver is performed after the ZP removing, where the N_s resulting symbols follow the same rule applied at the transmitter, being all reordered to obtain its original positions and therefore the OFDM based blocks, which can be written as,

$$\hat{\mathbf{x}}_B = \mathbf{\Pi}^{-1}\hat{\mathbf{x}}_{B\pi} \quad , \tag{2.16}$$

with $\hat{\mathbf{x}}_B$ being the set of OFDM based blocks $\hat{x}_{n,j}$ packed together with $j = 1, ..., N_s$ and $n = 1, ..., N$, $\hat{\mathbf{x}}_{B\pi}$ being the block of the resulting symbols, after the ZP removing, to be de-interleaved and $\mathbf{\Pi}$ the permutation

matrix based on the procedure described in the previous section. The following steps are similar to the BWB-OFDM technique.

2.4 CP-OFDM versus BWB-OFDM versus TIBWB-OFDM

This section presents an overall discussion of the CP-OFDM, BWB-OFDM [33] and TIBWB-OFDM [38] scheme when employing a MMSE [28] receiver, considering that the Figure 2.10 compares all these three approaches.

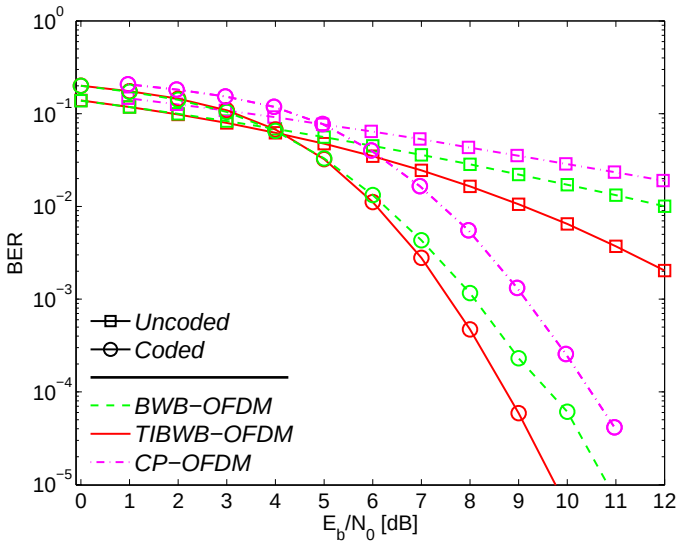

Figure 2.10: BER results for CP-OFDM, BWB-OFDM and TIBWB-OFDM, both coded and uncoded transmissions, over a severe time-dispersive channel [33] [38].

Firstly, the BWB-OFDM has much better performance for both coded and uncoded transmissions, presenting a gain of 2dB over a typical CP-OFDM when channel coding is used. This superior BER performance is achieved due to the use of a sole ZP rather than a CP and the use of a windowing technique, allowing to have a commitment between spectral confinement and transmission rate.

By comparing BWB-OFDM and TIBWB-OFDM, it is clear that the latter shows a considerable improvement towards the BWB-OFDM for both coded and uncoded transmissions, outperforming the BWB-OFDM by 1dB, approximately, when channel coding is used.

In comparison with BWB-OFDM, TIBWB-OFDM maintains the tradeoff between spectrum confinement and transmission rate as well as the PAPR level decrease, showing that this evolution is due to the time-interleaver approach that allows the receiver to recover corrupted data and consequently, handle with the deep fades of the time-dispersive channel successfully.

To conclude, the TIBWB-OFDM looks promising and for this reason, MIMO technique that will be discussed in the next chapters is combined with the TIBWB-OFDM in order to achieve a highly spectral and power efficient wireless system, while guaranteeing robustness against the multipath fading.

3 MIMO Systems

Next generation wireless communication systems are expected to support higher data rates. Note that this goal is particularly challenging for systems that are power, bandwidth and complexity limited. In SISO systems [44], the higher data rates can be reached by increasing either the transmission bandwidth or transmission power employing high order constellations, which is either expensive and/or leads to a huge consumption of mobile devices' battery, respectively.

MIMO wireless communication systems [25], which employs multiple antennas at both the transmitter and receiver, enables additional degrees of freedom to tackle this challenge, and improve both power and spectral efficiency. A MIMO system can provide a SD gain, a SM gain, as well as, an array gain [21]. Note that the array and diversity gains are not exclusive of MIMO systems, being also expected in single-input multiple-output (SIMO) and multiple-input single-output (MISO) systems [4]. For this reason, the SM gain is a unique characteristic of MIMO systems.

An increased reliability is achieved due to SD, by sending the same information through different antennas, while sharing the same channel and properly dealing with multipath fading characteristics of the wireless medium. On the other hand, higher data rates are attained by performing SM, in which information is split into several data streams, being sent in parallel through different transmit antennas, i.e. through different spatial channels. Furthermore, the required bandwidth remains the same, even with the increased throughput. However, those data rates are achieved at the cost of increased space requirements as a result of the higher number of antennas and significant increase of computation complexity required for multi-dimensional signal processing [16]. Finally, the array gain [34] denotes the improvement in the SNR at the receiver that results from a coherent combining effect of the wireless signals at the receiver. The coherent combining may be performed through spatial processing at the receive antenna array and/or spatial pre-processing at the transmit antenna array [4]. Thus, the resistance to noise is enhanced, improving the coverage of the wireless network.

In this way, MIMO technology has been widely studied and adopted by many wireless standards, including IEEE 802.11 [4], 802.16 [4], 3rd Groups Partnership Project (3GPP) [36], etc, as it offers an enhanced BER performance and higher data rates, improving the reliability and capacity of wireless systems [16].

3.1 System Model

Figure 3.1 depicts a MIMO system having N_T transmit and N_R receive antennas, whose channel can be described, at a given instant, by an $N_R \times N_T$ matrix $\mathbf{H} = \left[h_t^r\right]$, where h_t^r represents the channel gain between the t^{th} transmit and r^{th} receive antenna.

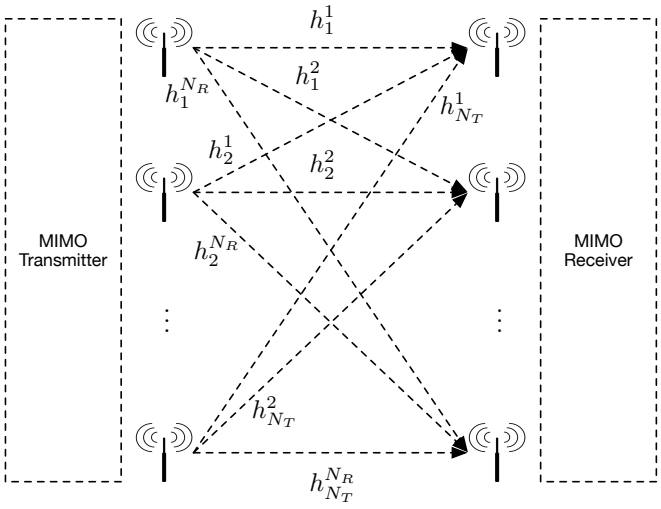

Figure 3.1: MIMO channel configuration.

In this case, the transmit antennas $T_1, ..., T_{N_T}$ send the signals $x_1, ..., x_{N_T}$, respectively, with each one being collected by all the receive antennas $R_1, ..., R_{N_R}$. The vector $\mathbf{y} = [y_1, ..., y_{N_r}]^T$ formed by the received signals at the N_R antennas with y_r denoting the signal received by r^{th} antenna is expressed as:

$$\mathbf{y} = \mathbf{H}\mathbf{x} + \mathbf{N} \Leftrightarrow \begin{bmatrix} y_1 \\ y_2 \\ \vdots \\ y_{N_R} \end{bmatrix} = \begin{bmatrix} h_1^1 & h_2^1 & \cdots & h_{N_T}^1 \\ h_1^2 & h_2^2 & \dots & h_{N_T}^2 \\ \vdots & \vdots & \ddots & \vdots \\ h_1^{N_R} & h_2^{N_R} & \dots & h_{N_T}^{N_R} \end{bmatrix} \begin{bmatrix} x_1 \\ x_2 \\ \vdots \\ x_{N_T} \end{bmatrix} + \begin{bmatrix} N_1 \\ N_2 \\ \vdots \\ N_{N_R} \end{bmatrix} \tag{3.1}$$

where $\mathbf{N}$ is the channel noise vector and $\mathbf{x}$ is the column vector with the signal transmitted.

The MIMO channel model can be considered either as wideband or narrowband, depending on how the effect of time dispersion is considered [12]. In other words, the narrowband system does not need to consider the time-dispersive nature of the channel, whereas the wideband system does. In this thesis only the wideband model will be considered, also known as frequency-selective channel model, in which different frequency components of the signal experience different attenuations and nonlinear phase shifts. From this point of view, MIMO systems seems less advantageous that SISO due to the number of transmitting signals, which increases the dimension of the channel matrix. However, the low correlation or even independence experienced between transmission paths (different pairs of transmitting and receiving antennas) and whose considered scenario is advantageous, i.e. the transmit and receive antennas spacing is sufficiently large [4], enables exploring SD or SM in MIMO, allowing for considerable gains in performance, either improved BER and/or higher throughput [29].

3.2 MIMO Techniques

In a wireless communication channel, the received signal power may suffer from severe random fluctuations in space and/or frequency and/or time. This random fluctuation in signal level, known as fading, can effect the quality and reliability of the communication system. Hence, it is extremely useful designing a system able to overcome this kind of impairments, namely the multipath fading.

For this purpose, two possible approaches able to deal multipath fading are presented in the next subsections, namely the SD and SM.

3.2.1 Spatial Diversity

Due to the time-dispersive nature of the mobile channel, it is essential to have a communication system able to deal with this problem. Spatial diversity technique [13] represents a possible approach, taken into consideration in a MIMO system. This technique is based on the transmission of multiple copies (ideally independent) of the signal over different paths between each pair of transmit and receive antennas. In this way, the system is redundant, in the sense that if a deep fade occurs in one of the paths, the information can still be recovered from the remaining paths. The Figure 3.2 illustrates how spatial diversity works in a MIMO system with $N_T = 3$ and $N_R = 3$, for sake of simplicity. Basically, the incoming data stream is replicated over the three different transmit antennas. These data streams are collected by all the receive antennas, i.e, each one will have a contribution from each transmitted data stream. Finally, it is up to receiver to obtain the original data stream, being guaranteed that at least one of the three transmitted data streams is received without any deep fade occurrence.

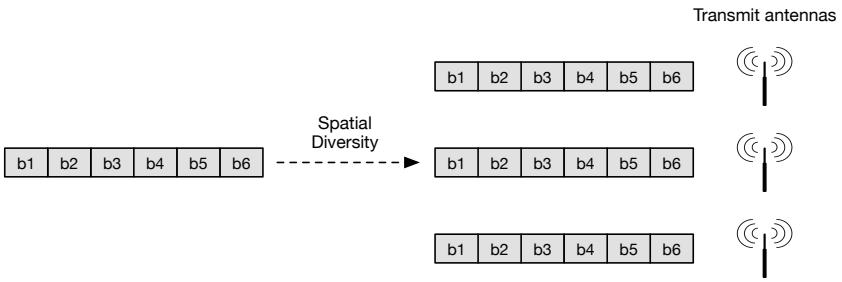

Figure 3.2: Spatial Diversity.

Consequently, in a system with N_T transmit and N_R receive antennas, the spatial diversity order [4] [21] is given by $N_T N_R$, which is the number of paths between the transmitter and receiver. The greater the diversity, the easier it is to deal with deep fading occurrences.

Therefore, SD technique is an effective method to deal with channel multipath fading, improving the quality (BER performance) and reliability of the system, even though the receiver complexity is increased, i.e. being necessary to have a receiver with a superior processing capability.

3.2.2 Spatial Multiplexing

SM is another approach, which exploits channel multipath fading rather than fight against it [21]. In order to SM works properly, the channel must have a significant amount of multipath scattering, even though fading occurrences are regarded as a way to degrade the conventional systems performance. The rich scattering verified in the propagation environment makes the channel spatially selective and therefore separable [29]. Hence, multiple data streams are created within the same frequency band to yield an increase in capacity. This increase in capacity come without any additional cost on bandwidth and power expenses. The data stream to be transmitted is divided into several parallel data streams which are transmitted simultaneously using the same frequency band.

Figure 3.3 illustrates how SM works in a MIMO system with $N_T = 3$ and $N_R = 3$, for sake of simplicity. Basically, the incoming data stream to be transmitted is separated into 3 (i.e number of transmit antennas N_T) independent lower rate data streams which are then simultaneously sent through the three transmit antennas. Note these three data streams occupy the same frequency band. These data streams are collected by all the receive antennas, i.e each one will have a contribution from each transmitted data streams. Since the environment is rich enough, the receiver can separate them and obtain the original data exploring the independence or low correlation between different transmit-receive paths. Furthermore, each data stream experiences at least the same channel quality that would be experienced by a SISO system, which increases the capacity by the number of streams. The separation mentioned previously determines the computational complexity of the receiver considered that will be discussed in Chapter 4.

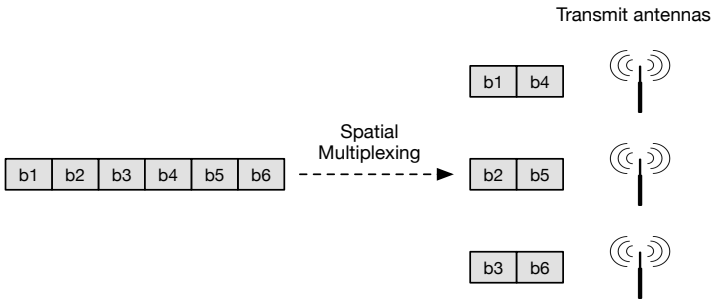

Figure 3.3: Spatial Multiplexing.

As a result, the SM gain is given by $min\{N_T,N_R\}$, which is also the number of streams that can be reliably supported by a MIMO Channel [4]. This condition shows that the throughput increases with the number of antennas of the system. Moreover, the number of the streams also increases, not requiring a wider bandwidth, which improves significantly the spectral efficiency [5], as well as, the channel capacity.

Assuming that the channel is known at both the transmitter and the receiver side, it is shown in [19] and [40] that the capacity of the MIMO system with $min\{N_T,N_R\}$ links can be given by

$$C = \max_{Tr(\mathbf{R}_{xx})=N_T} \left\{ \log_2 \left[det(\mathbf{I}_{N_R} + \frac{SNR}{N_T}\mathbf{H}\mathbf{R}_{xx}\mathbf{H}^H) \right] \right\} \tag{3.2}$$

where $Tr()$ and $det()$ denotes the trace and determinant of a matrix, respectively, and, $\mathbf{R}_{xx}$ is the autocorrelation matrix of the transmitted signal, $\mathbf{I}_{N_R}$ is an identity matriz with size N_R, SNR denotes the overall signal to noise ratio of the system and $\mathbf{H}^H$ denotes the Hermitian of the channel information matrix $\mathbf{H}$. Most of the times, $\mathbf{R}_{xx}$ is represented by a diagonal matrix as the transmitted signals are independent, being considered as the power distribution among the transmitters.

Note that, there are situations where a MIMO system can achieve both diversity and multiplexing gains, simultaneously [4]. However, it is critical to have a commitment between these two gains. Thus, in order to reach a higher spatial diversity gain, the spatial multiplexing gain must be lowered, and vice versa [43] [27].

Since this thesis focuses on the increase of the spectral efficiency and the throughput of the system, the SM approach will be considered in the following chapters.

4 MIMO-OFDM System

OFDM provides a robustness against frequency selective fading by splitting a frequency-selective channel into several narrowband flat fading sub-channels. Hence, each symbol or set of symbols from the incoming bitstream is transmitted over those parallel sub-carriers, providing a simple channel equalisation, which reduces significantly the equaliser complexity for each subcarrier [33]. Furthermore, the orthogonality between the subcarriers that carried the transmitted signals and its overlapping spectrums yields a superior spectral efficiency. Hence, this multi-carrier technique represents a good choice for high data rate wireless transmission. On the other hand, MIMO brings either enhanced BER performance or higher data rates (hence, increased spectral efficiency) for wireless communications, through the use of SD or SM techniques, respectively. In this case, SM is considered which means that MIMO exploits the channel multipath fading, since its separability relies on the presence of rich multipath fading [21].

By combining MIMO and OFDM techniques, an improved high speed wireless communication system is achieved, being denoted as MIMO-OFDM. This system provides an increased capacity, and consequently, higher data rates, as well as, improved spectral efficiency. Although, MIMO-OFDM represents an attractive solution for enhancing the data rates of a communication system operating over frequency-selective fading channels and dealing with multipath propagation scenarios, it also presents considerable challenges, namely due to the additional receiver complexity, result of the required channel matrix inversions.

4.1 System Model

The schematic block diagram of the MIMO-OFDM system with N_T transmit, N_R receive antennas and N subcarriers is illustrated in Figure 4.1.

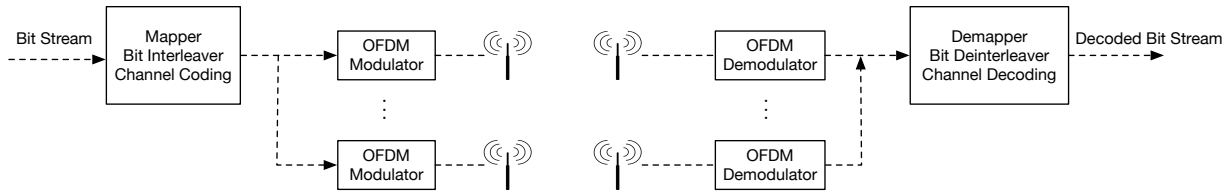

Figure 4.1: MIMO-OFDM System.

The original bit stream is mapped into a selected M-ary signal constellation. Before being the OFDM modulation performed, channel coding and bit interleaving are applied to the considered bit stream in order to ensure a robust transmission over the MIMO frequency-selective channel. Hence, each transmit antenna has a related OFDM symbol, which is sent through the mentioned channel, whose impairments are

handled by the employment of SM. The frequency domain received signal $Y_k^{(r)}$:$\{k = 0, 1, ..., N-1\}$, with $r = 0, ..., N_R - 1$, on the k^{th} subcarrier can be represented by

$$\mathbf{Y}_k = [Y_k^{(1)}, ..., Y_k^{(N_R)}]^T = \mathbf{H}_k \mathbf{X}_k + \mathbf{N}_k \quad , \tag{4.1}$$

where $\mathbf{X}_k = [X_{k,(1)}, ..., X_{k,(N_T)}]^T$ and $\mathbf{N}_k = [N_k^{(1)}, ..., X_k^{(N_R)}]^T$ denotes the transmitted signal and the channel noise in frequency domain, respectively, and $\mathbf{H}_k$ represents the overall channel frequency response that can be given by the following matrix,

$$\mathbf{H}_k = \begin{bmatrix} H_{k,(1)}^{(1)} & H_{k,(2)}^{(1)} & \cdots & H_{k,(N_T)}^{(1)} \\ H_{k,(1)}^{(2)} & H_{k,(2)}^{(2)} & \cdots & H_{k,(N_T)}^{(2)} \\ \vdots & \vdots & \ddots & \vdots \\ H_{k,(1)}^{(N_R)} & H_{k,(2)}^{(N_R)} & \cdots & H_{k,(N_T)}^{(N_R)} \end{bmatrix} \quad , \tag{4.2}$$

with $H_{k,(t)}^{(r)}$, with $t = 0, ..., N_T - 1$, being the channel between the t^{th} transmit antenna and the r^{th} receive antenna for the k^{th} subcarrier.

At the receiver side, in order to achieve the original bit stream, the OFDM symbols are demodulated, followed by bit de-interleaving and channel decoding.

4.2 Equalisation Techniques

As previously stated, in order to achieve low complexity equalisation of the frequency-selective channel with increased capacity, OFDM and MIMO techniques are combined. Consequently, a flat fading channel is assumed over each sub-carrier, enabling fast forward implementation of a linear frequency domain equalisation with ISI suppression maintaining the simplicity of the equaliser at an affordable cost of some increased complexity.

The ZF and MMSE techniques [9], which decouples the received signals into uncorrelated signals, can be used in MIMO-OFDM. These linear equalisers require channel matrix inversions, which is disadvantageous for the regarded system, since the computational complexity increases enormously with the number of transmit and receive antennas.

The receiver simplicity can be kept by employing the EGC [2] [6] [14] and MRC [2] [6], which do not require matrix inversions. However, the residual interference levels (both ISI and the interference between different transmitted streams) can be too high with such low complexity receivers [2] [14]. For this reason, the aforementioned techniques should be made iterative while still seeing performed in the frequency domain, in such a way that from one iteration to another the residual interference levels is being removed.

4.2.1 Zero Forcing

The ZF [22] is one of the most known methods to equalise and/or perform signal separation. The idea behind this simple technique is to invert the channel matrix $\mathbf{H}$. In the case of a singular channel matrix, ZF uses the Moore-Penrose pseudo inverse matrix approach [35], known also as ZF receiver matrix, defined as

follows,

$$\mathbf{G}_k = (\mathbf{H}_k^H \mathbf{H}_k)^{-1} \mathbf{H}_k^H \quad , \tag{4.3}$$

with $\mathbf{H}_k^H$ being the Hermitian matrix of $\mathbf{H}_k$.

Considering (4.1), the estimated signal $\tilde{\mathbf{X}}_k = [\tilde{X}_{k,(1)}, ..., \tilde{X}_{k,(N_T)}]^T$ is given by,

$$\begin{aligned} \tilde{\mathbf{X}}_k &= \mathbf{G}_k \mathbf{Y}_k \\ &= \mathbf{G}_k \mathbf{H}_k \mathbf{X}_k + \mathbf{G}_k \mathbf{N}_k \\ &= (\mathbf{H}_k^H \mathbf{H}_k)^{-1} (\mathbf{H}_k^H \mathbf{H}_k) \mathbf{X}_k + \mathbf{G}_k N_k \\ &= \mathbf{X}_k + \mathbf{G}_k \mathbf{N}_k \quad . \end{aligned} \tag{4.4}$$

The ZF method not only allows perfect separation of different users or different transmitted data streams, but also cancels all ISI. In other words, for each receiver antenna, the contributions from other antennas are null, working well in interference-limited scenarios. However, as it disregards the effect of noise from the overall design and focuses only on perfect removing the interference term from $\mathbf{X}_k$, it can have severe noise enhancement, working poorly under noise-limited scenarios [32]. In addition, the inversion of high dimension matrices increases the ZF implementation complexity.

4.2.2 Minimum Mean Squared Error

The MMSE receiver aims to obtain the estimated signals $\tilde{\mathbf{X}}_k = [\tilde{X}_{k,(1)}, ..., \tilde{X}_{k,(N_T)}]^T$, through minimising the mean squared error, $E\{(\tilde{\mathbf{X}}_k - \mathbf{X}_k)(\tilde{\mathbf{X}}_k - \mathbf{X}_k)^H\}$, whose matrix solution [9] is given by,

$$\mathbf{G}_k = \left(\mathbf{H}_k^H \mathbf{H}_k + \frac{1}{SNR} \mathbf{I}_{N_T} \right)^{-1} \mathbf{H}_k^H \quad , \tag{4.5}$$

where the SNR is σ_x^2/σ_η^2 with σ_x^2 and σ_η^2 being the power of the transmitted signals and noise respectively, $\mathbf{H}_k^H$ the Hermitian matrix of $\mathbf{H}_k$ and $\mathbf{I}_{N_T}$ an identity matrix with size N_T.

Considering (4.1), the estimated signal $\tilde{\mathbf{X}}_k = [\tilde{X}_{k,(1)}, ..., \tilde{X}_{k,(N_T)}]^T$ is given by:

$$\begin{aligned} \tilde{\mathbf{X}}_k &= \mathbf{G}_k \mathbf{Y}_k \\ &= \mathbf{G}_k \mathbf{H}_k \mathbf{X}_k + \mathbf{G}_k \mathbf{N}_k \quad . \end{aligned} \tag{4.6}$$

A trade-off between noise enhancement and ISI mitigation (interference) is achieved by the MMSE equaliser, which considers the noise term in the design of its $\mathbf{G}_k$ matrix. Thus, the BER performance is improved in comparison with the ZF equaliser. Nevertheless, it also requires inversion of high dimension matrices, increasing its complexity. Moreover, through (4.6) it is shown that at high SNR regime, MMSE converges to ZF solution.

4.2.3 Maximum Ration Combiner

The MRC equaliser combines the individually received branch signals so as to maximize the received SNR [22]. More specifically, the received signals are phased corrected and weighted by the conjugate of the

channel matrix, being the combined SNR the sum of the received signals SNRs [15]. Thus, the received SNR grows with the number of receive antennas, being the detection of the transmitted signals less complicated. The MRC receiver G_k at the k^{th} subcarrier is given by,

$$\mathbf{G}_k = \mathbf{H}_k^* \quad , \tag{4.7}$$

with $\mathbf{H}_k^*$ being the conjugate of the channel matrix $\mathbf{H}_k$.

Considering (4.1), the estimated signal $\tilde{\mathbf{X}}_k = [\tilde{X}_{k,(1)}, ..., \tilde{X}_{k,(N_T)}]^T$ is given by:

$$\begin{aligned} \tilde{\mathbf{X}}_k &= \mathbf{G}_k \mathbf{Y}_k \\ &= \mathbf{G}_k \mathbf{H}_k \mathbf{X}_k + \mathbf{G}_k \mathbf{N}_k \\ &= \mathbf{H}_k^* \mathbf{H}_k \mathbf{X}_k + \mathbf{H}_k^* \mathbf{N}_k \\ &= |\mathbf{H}_k|^2 \mathbf{X}_k + \mathbf{H}_k^* \mathbf{N}_k \quad . \end{aligned} \tag{4.8}$$

Although the MRC is optimal in sense of SNR, this technique requires the weights to vary with the magnitude of the received signals that may fluctuate due to the multipath propagation in the wireless communications. Furthermore, since MRC does not require channel matrix inversion, the channel effects are not completely removed, worsening the ISI effect. In this way, the interference levels (both ISI and interference between different transmitted streams) are substantial, being an excellent equaliser for scenarios with high values of N_R/N_T, where MRC is able to efficiently separate the received data streams [2] [6].

4.2.4 Equal Gain Combiner

Unlike MRC, which requires the computation of the conjugate of the channel matrix, EGC only involves phase rotations, combining all the signals associated to the different receive antennas with unitary weights to achieve a high SNR [22]. Hence, the matrix $\mathbf{A_k}$ is obtained from $\mathbf{H}_k$, where the (r,t)-th element of $\mathbf{A_k}$ is given by,

$$A_{k,(t)}^{(r)} = e^{(jarg(H_{k,(t)}^{(r)}))} \quad , \tag{4.9}$$

i.e, they have value 1 and phase identical to the corresponding element of the matrix $\mathbf{H_k}$, being the EGC receiver matrix at the k^{th} subcarrier given by,

$$\mathbf{G}_k = \mathbf{A}_k^* \quad . \tag{4.10}$$

Considering (4.1), the estimated signal $\tilde{\mathbf{X}}_k = [\tilde{X}_{k,(1)}, ..., \tilde{X}_{k,(N_T)}]^T$ is given by:

$$\begin{aligned} \tilde{\mathbf{X}}_k &= \mathbf{G}_k \mathbf{Y}_k \\ &= \mathbf{G}_k \mathbf{H}_k \mathbf{X}_k + \mathbf{G}_k \mathbf{N}_k \\ &= \mathbf{A}_k^* \mathbf{H}_k \mathbf{X}_k + \mathbf{A}_k^* \mathbf{N}_k \quad . \end{aligned} \tag{4.11}$$

Similar to MRC, the EGC method does not require channel matrix inversion. Thus, the channel effects are not completely removed, having therefore a high ISI effect associated besides the interference between

transmitted streams. Moreover, the EGC sets all the received signals with unitary gain. In this way, unlike MRC, the ISI is not worsened, being an excellent equaliser for intermediate scenarios, i.e, with moderate values of N_R and N_T [2] [6] [14].

4.2.5 Iterative Receivers

The use of simple techniques to separate data streams that avoid matrix inversions to keep the receiver complexity low is very desired. However, techniques such as EGC and MRC have as drawback an increased in ISI effect and of interference between transmitted streams. An improved solution is the use of iterative frequency domain receivers based on EGC and MRC, employing N_R frequency-domain feedforward filters (one for each receive antenna) and N_T frequency-domain feedback filters (one for each transmit antenna) [2] [6] [14]. The feedforward filters equalise the channel effects, assuming perfect channel knowledge; whereas the feedback filters try to remove the ISI and the residual interference between the different transmitted streams (for the first iteration those terms are zero), taking into account previous estimations. In other words, the interferences cancellation depends on the reliability of the estimated data at the previous iterations. The basic scheme followed by both EGC and MRC iterative receivers for detection of the signal transmitted by each transmit antenna, at the l^{th} iteration, is presented in Figure 4.2.

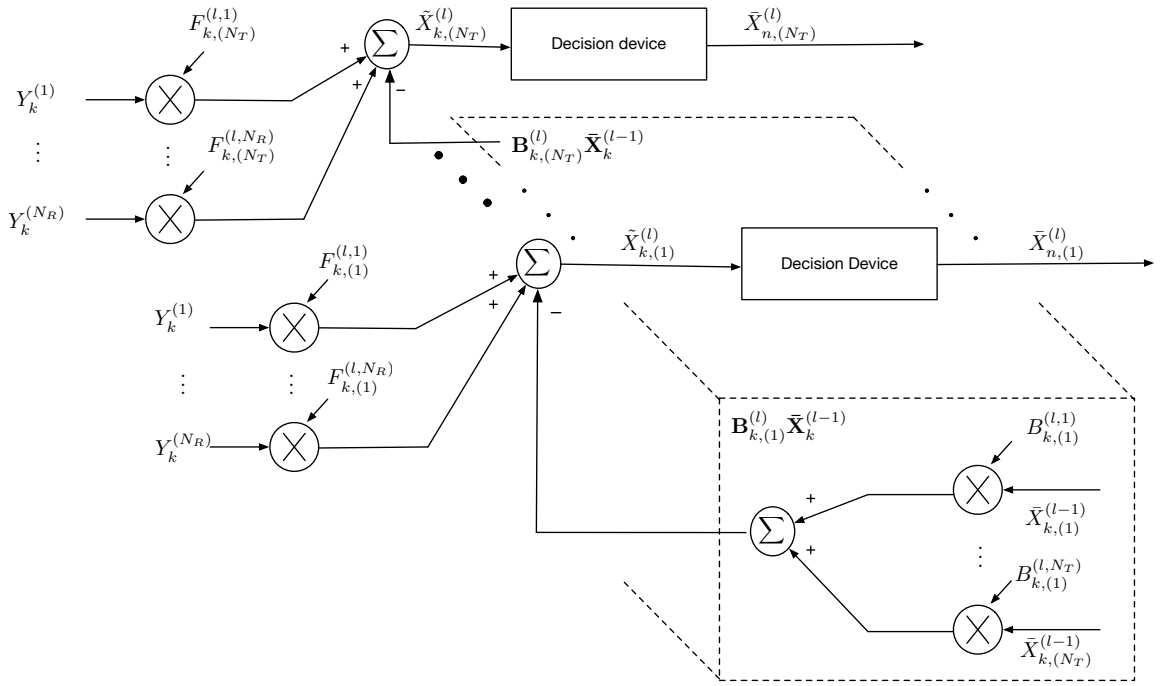

Figure 4.2: Block diagram representation for detection of the N_T transmitted signals, at the l^{th} iteration.

Considering (4.1), at the l^{th} iteration, the estimated signal $\tilde{\mathbf{X}}^{(l)}_k = [\tilde{X}^{(l)}_{k,(1)}, ..., \tilde{X}^{(l)}_{k,(N_T)}]^T$ in the frequency domain, at the k^{th} subcarrier is given by,

$$\tilde{\mathbf{X}}^{(l)}_k = \mathbf{F}^{(l)T}_k \mathbf{Y}_k - \mathbf{B}^{(l)T}_k \bar{\mathbf{X}}^{(l-1)}_k \quad , \tag{4.12}$$

where the feedforward and feedback matrices are, respectively,

$$\mathbf{F}_k^{(l)} = \begin{bmatrix} F_{k,(1)}^{(l,1)} & F_{k,(2)}^{(l,1)} & \cdots & F_{k,(N_T)}^{(l,1)} \\ F_{k,(1)}^{(l,2)} & F_{k,(2)}^{(l,2)} & \cdots & F_{k,(N_T)}^{(l,2)} \\ \vdots & \vdots & \ddots & \vdots \\ F_{k,(1)}^{(l,N_R)} & F_{k,(2)}^{(l,N_R)} & \cdots & F_{k,(N_T)}^{(l,N_R)} \end{bmatrix} \tag{4.13}$$

and

$$\mathbf{B}_k^{(l)} = \begin{bmatrix} B_{k,(1)}^{(l,1)} & B_{k,(2)}^{(l,1)} & \cdots & B_{k,(N_T)}^{(l,1)} \\ B_{k,(1)}^{(l,2)} & B_{k,(2)}^{(l,2)} & \cdots & B_{k,(N_T)}^{(l,2)} \\ \vdots & \vdots & \ddots & \vdots \\ B_{k,(1)}^{(l,N_T)} & B_{k,(2)}^{(l,N_T)} & \cdots & B_{k,(N_T)}^{(l,N_T)} \end{bmatrix} \tag{4.14}$$

where $F_{k,(t)}^{(l,r)}$ and $B_{k,(t)}^{(l,t)}$ are the feedforward and feedback filters coefficients for the l^{th} iteration and the vector $\bar{\mathbf{X}}_k^{(l-1)} = [\bar{X}_{k,(1)}^{(l-1)}, ..., \bar{X}_{k,(N_T)}^{(l-1)}]^T$ containing frequency-domain estimated of the transmitted signals values obtained at the previous iteration $(l-1)$ at the output receiver.

In order to explain the scheme presented in Figure 4.2, let consider the transpose of the $\mathbf{F}_k^{(l)}$ and $\mathbf{B}_k^{(l)}$ given by

$$\mathbf{F}_k^{(l)T} = \begin{bmatrix} F_{k,(1)}^{(l,1)} & F_{k,(1)}^{(l,2)} & \cdots & F_{k,(1)}^{(l,N_R)} \\ F_{k,(2)}^{(l,1)} & F_{k,(2)}^{(l,2)} & \cdots & F_{k,(2)}^{(l,N_R)} \\ \vdots & \vdots & \ddots & \vdots \\ F_{k,(N_T)}^{(l,1)} & F_{k,(N_T)}^{(l,2)} & \cdots & F_{k,(N_T)}^{(l,N_R)} \end{bmatrix} \tag{4.15}$$

and

$$\mathbf{B}_k^{(l)T} = \begin{bmatrix} B_{k,(1)}^{(l,1)} & B_{k,(1)}^{(l,2)} & \cdots & B_{k,(1)}^{(l,N_T)} \\ B_{k,(2)}^{(l,1)} & B_{k,(2)}^{(l,2)} & \cdots & B_{k,(2)}^{(l,N_T)} \\ \vdots & \vdots & \ddots & \vdots \\ B_{k,(N_T)}^{(l,1)} & B_{k,(N_T)}^{(l,2)} & \cdots & B_{k,(N_T)}^{(l,N_T)} \end{bmatrix} \tag{4.16}$$

Thus, the first and second parcel of (4.12) can also be represented as, respectively,

$$\mathbf{F}_k^{(l)T}\mathbf{Y}_k = \begin{cases} F_{k,(1)}^{(l,1)}Y_k^{(1)} + F_{k,(1)}^{(l,2)}Y_k^{(2)} + \cdots + F_{k,(1)}^{(l,N_R)}Y_k^{(N_R)} \\ F_{k,(2)}^{(l,1)}Y_k^{(1)} + F_{k,(2)}^{(l,2)}Y_k^{(2)} + \cdots + F_{k,(2)}^{(l,N_R)}Y_k^{(N_R)} \\ \vdots \\ F_{k,(N_T)}^{(l,1)}Y_k^{(1)} + F_{k,(N_T)}^{(l,2)}Y_k^{(2)} + \cdots + F_{k,(N_T)}^{(l,N_R)}Y_k^{(N_R)} \end{cases} \tag{4.17}$$

and

$$\mathbf{B}_k^{(l)T}\bar{\mathbf{X}}_k^{(l-1)} = \begin{cases} B_{k,(1)}^{(l,1)}\bar{X}_{k,(1)}^{(l-1)} + B_{k,(1)}^{(l,2)}\bar{X}_{k,(2)}^{(l-1)} + \cdots + B_{k,(1)}^{(l,N_T)}\bar{X}_{k,(N_T)}^{(l-1)} \\ B_{k,(2)}^{(l,1)}\bar{X}_{k,(1)}^{(l-1)} + B_{k,(2)}^{(l,2)}\bar{X}_{k,(2)}^{(l-1)} + \cdots + B_{k,(2)}^{(l,N_T)}\bar{X}_{k,(N_T)}^{(l-1)} \\ \vdots \\ B_{k,(N_T)}^{(l,1)}\bar{X}_{k,(1)}^{(l-1)} + B_{k,(N_T)}^{(l,2)}\bar{X}_{k,(2)}^{(l-1)} + \cdots + B_{k,(N_T)}^{(l,N_T)}\bar{X}_{k,(N_T)}^{(l-1)} \end{cases} \tag{4.18}$$

where the t^{th} row of (4.17) and (4.18) refers to each parcel in order to achieve the detected signal transmitted

by the t^{th} antenna. Therefore, at the l^{th} iteration, the detection of the first transmitted message can be given by,

$$\begin{aligned}\tilde{\mathbf{X}}_{k,(1)}^{(l)} &= (F_{k,(1)}^{(l,1)}Y_k^{(1)} + F_{k,(1)}^{(l,2)}Y_k^{(2)} + \cdots + F_{k,(1)}^{(l,N_R)}Y_k^{(N_R)}) \\ &\quad - (B_{k,(1)}^{(l,1)}\bar{X}_{k,(1)}^{(l-1)} + B_{k,(1)}^{(l,2)}\bar{X}_{k,(2)}^{(l-1)} + \cdots + B_{k,(1)}^{(l,N_T)}\bar{X}_{k,(N_T)}^{(l-1)}) \quad .\end{aligned} \tag{4.19}$$

Being the detection of the N_T^{th} transmitted message given by,

$$\begin{aligned}\tilde{\mathbf{X}}_{k,(N_T)}^{(l)} &= F_{k,(N_T)}^{(l,1)}Y_k^{(1)} + F_{k,(N_T)}^{(l,2)}Y_k^{(2)} + \cdots + F_{k,(N_T)}^{(l,N_R)}Y_k^{(N_R)} \\ &\quad - B_{k,(N_T)}^{(l,1)}\bar{X}_{k,(1)}^{(l-1)} + B_{k,(N_T)}^{(l,2)}\bar{X}_{k,(2)}^{(l-1)} + \cdots + B_{k,(N_T)}^{(l,N_T)}\bar{X}_{k,(N_T)}^{(l-1)} \quad .\end{aligned} \tag{4.20}$$

Since the interference levels can still be substantial for both linear MRC and EGC methods, especially for moderate values of N_R/N_T, an iterative receiver based on each mentioned method is proposed in [2] [6] [14], in which the first iteration corresponds to linear frequency domain equalisation/signal separation described in the Subsections 4.2.3 and 4.2.4, following the scheme of the Figure 4.2.

Maximum Ratio Combiner

For the iterative MRC receiver, the estimated signal can be also represented by (4.12), whose feedforward filter and feedback filter can be given by, respectively, [2]

$$\begin{aligned}\mathbf{F}_k^T &= \kappa\mathbf{H}_k^H \\ \mathbf{B}_k^T &= \mathbf{F}_k^T\mathbf{H}_k - \mathbf{I}_{N_T} = \kappa\mathbf{H}_k^H\mathbf{H}_k - \mathbf{I}_{N_T} \quad ,\end{aligned} \tag{4.21}$$

where the normalisation parameter κ denotes the diagonal normalisation matrix whose (t,t)th element, being recalculated in each iteration and given by,

$$\kappa = \left(\sum_{k=0}^{N-1} \sum_{r=1}^{N_R} \left| F_{k,(t)}^{(l,r)T} H_{k,(t)}^{(r)} \right|^2 \right)^{-1} \quad . \tag{4.22}$$

The expressions of $\mathbf{B}_k^T$ and κ are easy to understand when considering the first iteration of the method, and the fact that the matrix $\mathbf{F}_k^{(0)T}\mathbf{H}_k = \mathbf{H}_k^H\mathbf{H}_k$ is not unitary, and as seen for ZF and MMSE it would be desired to approximate the product $\mathbf{F}_k^{(0)T}\mathbf{H}_k$ to or close to an unitary one while minimising the mean square error. For this reason, the diagonal normalisation matrix κ is crucial to ensure that $\kappa\mathbf{H}_k^H\mathbf{H}_k \approx N_T\mathbf{I}$ [2]. Moreover, the matrix $\mathbf{B}_k$ accounts the interference cancellation, which means that as the number of iterations increases, its coefficients tend to null values.

Equal Gain Combiner

For the iterative EGC receiver, the estimated signal can be represented by (4.12), whose feedforward filter and feedback filter can be given by, respectively,

$$\begin{aligned} \mathbf{F}_k^T &= \kappa \mathbf{A}_k^H \\ \mathbf{B}_k^T &= \mathbf{F}_k^T \mathbf{H}_k - \mathbf{I}_{N_T} = \kappa \mathbf{A}_k^H \mathbf{H}_k - \mathbf{I}_{N_T} \quad , \end{aligned} \tag{4.23}$$

where the normalisation parameter κ denotes the diagonal normalisation matrix whose (t,t)th element, being recalculated in each iteration as well and given by,

$$\kappa = \left(\sum_{k=0}^{N-1} \sum_{r=1}^{N_R} \left| F_{k,(t)}^{(l,r)T} H_{k,(t)}^{(r)} \right| \right)^{-1} \quad . \tag{4.24}$$

The argument considered in the MRC method is analogous to the EGC method, being therefore κ and $\mathbf{B}_k^T$ used for the same goal. The only difference is in the matrix $\mathbf{F}_k^{(0)T} \mathbf{H}_k$ that, in this case, is given by $\mathbf{A}_k^H \mathbf{H}_k$. Hence, the diagonal normalisation matrix κ is essential to guarantee that $\kappa \mathbf{A}_k^H \mathbf{H}_k \approx N_T \mathbf{I}$ [2] [14].

5 Spatially Multiplexed MIMO Time Interleaved BWB-OFDM Systems

A MIMO system with N_T transmit antennas and N_R receive antennas operating in both uplink and downlink can be considered as a single-user MIMO (SU-MIMO) or a multi-user MIMO (MU-MIMO) [20].

A SU-MIMO system [4], illustrated in the Figure 5.1, considers a single multiple-antenna transmitter communicating with a single multiple-antenna receiver, consisting of one user equipped with N_T antennas and one base station (BS) equipped with $N_R \geq N_T$ antennas, respectively. Spatial Diversity or Spatial Multiplexing or even a combination of these two techniques can be employed to achieve an increased reliability or higher data rates or a commitment between these two characteristics, respectively.

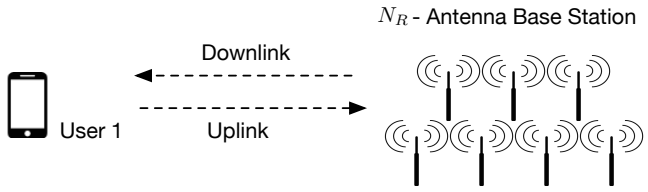

Figure 5.1: Single-User MIMO system.

A MU-MIMO system [10], illustrated in the Figure 5.2, considers multiple users communicating with a multiple antenna BS. In this case, the BS is equipped with N_R antennas, while each user has a single antenna, although each user can also be equipped with multiple antennas, in a more general MU-MIMO scenario [32]. Similar to SU-MIMO, MU-MIMO can achieve either multiplexing gain or a diversity gain or even a commitment between these two gains, depending on the MIMO tecnique employed.

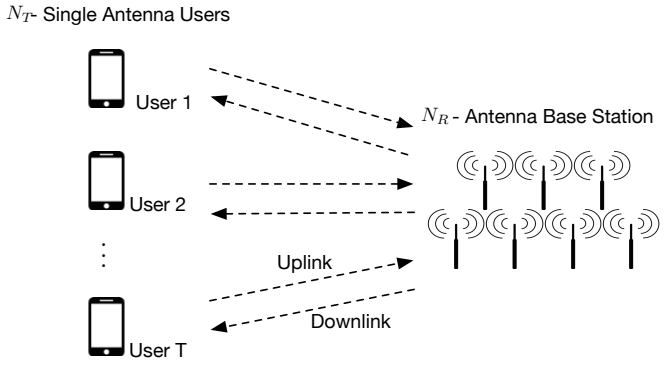

Figure 5.2: Diagram of a Multi-User MIMO System.

In this chapter a SU-MIMO scheme will be combined with the SM technique in an uplink scenario, presented in Figure 5.3, since one of the interests of this thesis is to increase the throughput of system. For this reason, under suitable channel conditions, such as rich scattering in the environment, SM is employed, increasing the data rate of the user and, consequently, the channel capacity, which provides at most $min\{N_T,N_R\}$ spatial degrees of freedom.

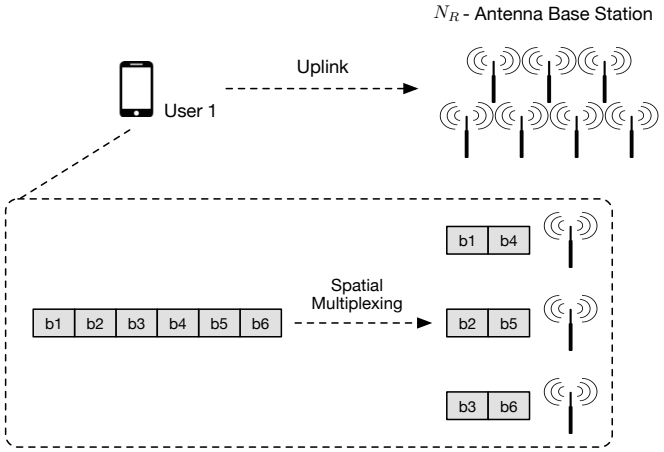

Figure 5.3: Diagram of a Single-User MIMO System employing SM for an uplink scenario.

The main focus of this chapter will be the combination of the SU-MIMO approach employing SM with the TIBWB-OFDM technique [38], described in Section 2.3, achieving a new highly spectral and power efficient wireless communication system. More specifically, this new system combines the higher data rates provided by use of SM technique with the improved spectral and power efficiency of TIBWB-OFDM (which enables either higher data rates or better spectrum confinement), allowing therefore for a considerable enhance in spectral efficiency, while guaranteeing robustness against the deep fades of the frequency selective MIMO channel. Furthermore, it presents better power efficiency than conventional MIMO-OFDM because of the elimination of a CP per transmitted OFDM symbol.

5.1 Transmitter

For the purpose of describing the MIMO TIBWB-OFDM transmitter, Figure 5.4, consider a sequence of modulated symbols, resulting form direct mapping of a incoming binary sequence into a selected constellation (e.g. quadrature phase shift keying (QPSK)). In order to ensure a robust transmission, channel coding and bit interleaving are applied to the considered incoming binary sequence, prior to modulation.

The SM technique is performed and based on the Figure 3.3, the modulated symbols are divided into N_T low-rate sub-streams, each one associated with one transmit antenna, being denoted as $S_k^{(t)}$:$\{k = 0, 1, ..., N-1\}$ with $t = 1, ..., N_T$, and where it is considered that each TIBWB-OFDM employs OFDM blocks with N subcarriers. A robustness against deep frequency fades combined with the superior both spectral and power efficiency is guaranteed by performing the TIBWB-OFDM technique [38] (whose scheme was presented in the Figure 2.8 and explained in detail in the Subsection 2.3.1) in each spatial stream $S_k^{(t)}$ with $t = 0, ..., N_T - 1$. In essence, taking as example the t^{th} spatial stream, each OFDM block, in the time domain, i.e. $s_n^{(t)} = \text{IDFT}_N\{S_k^{(t)}\}$, with $k = 0, ..., N-1$ and $n = 0, ..., N-1$, is cyclic extended in order to be windowed by

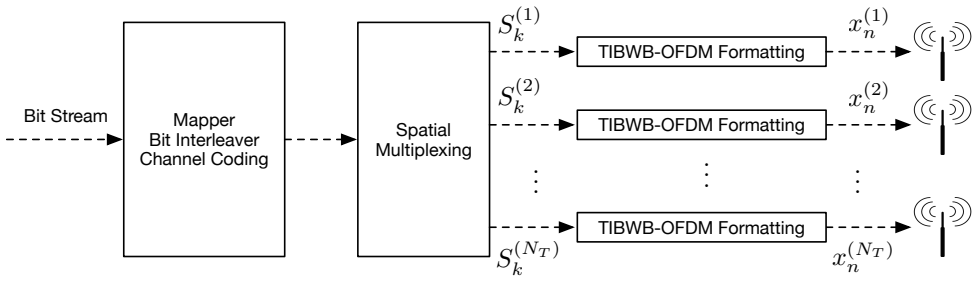

Figure 5.4: MIMO TIBWB-OFDM transmitter scheme.

a smoother, non-rectangular window and hence allowing a better spectrum confinement at the cost of an increase of the samples per transmitted symbol. After that, the contents of this processed spectral shaped OFDM blocks, packed in groups of N_s blocks, are time-interleaved between each other, resulting in N_s interleaved block of symbols (see Figure 2.8), creating a kind of diversity effects at the frequency domain, and consequently, allowing to better overcome the deep fades noticed in the wireless channels. Finally, to cope with a time-dispersive multipath channel, a sole ZP guard interval is appended at the end of the reassembled block, being the TIBWB-OFDM symbol transmitted at the t^{th} transmit antenna denoted as $x_{n,(t)}$:$\{n = 0, 1, ..., N_x - 1\}$.

5.2 Receiver

The MIMO TIBWB-OFDM receiver is presented in Figure 5.5. Its main role is to equalise the N_R received signals and perform the unformatting of TIBWB-OFDM estimated symbols [38], where time-deinterleaving and matched filtering are performed in order to suppress the ACI at each spatial data stream.

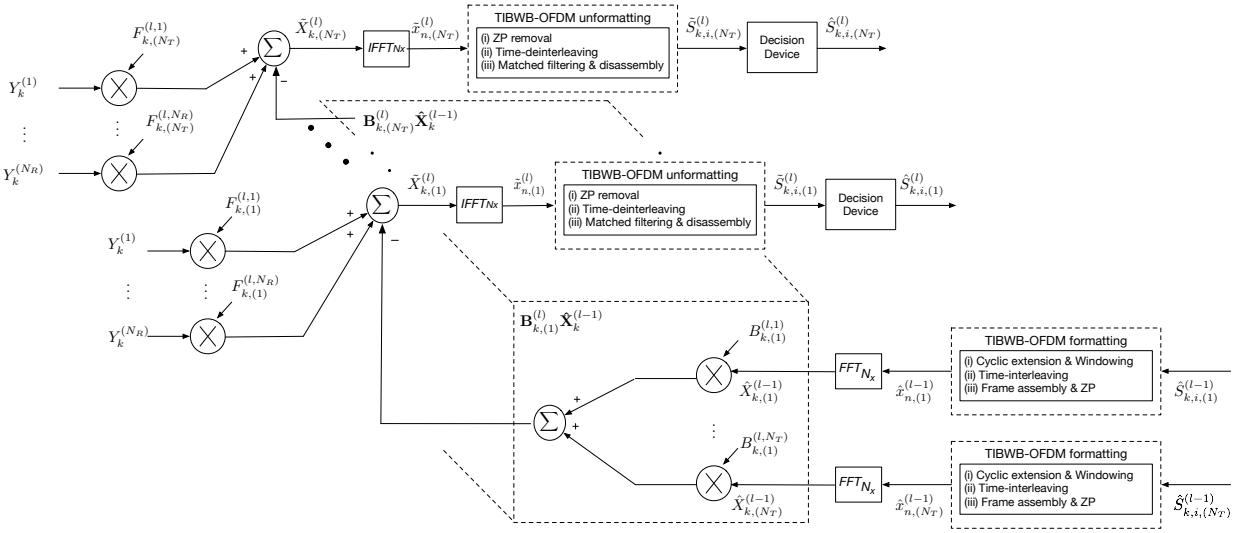

Figure 5.5: MIMO TIBWB-OFDM Receiver Scheme with Iterative Frequency Domain Equalisation.

The received signal at the r^{th} receive antenna $y_n^{(r)}$:$\{n = 0, 1, ..., N_x - 1\}$ is first converted to the frequency domain resulting in $Y_k^{(r)}$:$\{k = 0, 1, ..., N_x - 1\}$ by performing a N_x-sized discrete fourier transform (DFT) (implemented through the efficient FFT algorithm)[1]. When assuming that the chosen duration of the guard

[1]Remember that the size of each TIBWB-OFDM symbol is $N_x = N_{ZP} + N_s \times N(1 + \beta)$. Refer to section 2.3 for further details.

interval is longer than the duration of the channel impulse response, the vector $\mathbf{Y}_k$ of frequency domain samples at the k^{th} carrier for all receive antennas, with $k = 0, 1, ..., N_x - 1$, can be written as

$$\mathbf{Y}_k = \left[Y_k^{(1)}, ..., Y_k^{(N_R)} \right]^T = \mathbf{H}_k \mathbf{X}_k + \mathbf{N}_k \quad , \tag{5.1}$$

with $\mathbf{X}_k = [X_{k,(1)}, ..., X_{k,(N_T)}]^T$ and $X_{k,(t)} = \mathrm{DFT}_{N_x}\{x_{n,(t)}\}$, with $k = 0, ..., N_x - 1$, $n = 0, ..., N_x - 1$, and $t = 0, ..., N_T - 1$. $\mathbf{H}_k$ and $\mathbf{N}_k$ denote, at the k^{th} subcarrier, the $N_R \times N_T$ channel matrix (with $(r, t) - th$ element denoted by $H_{k,(t)}^{(r)}$, similar to (4.2)) and the channel noise matrix, respectively.

Then, it follows equalisation, which can be performed with one of the previously discussed equalisers: MMSE, ZF, EGC and MRC. Receivers employing MMSE or ZF are linear FDEs while iterative receivers based on EGC and MRC concepts are nonlinear. Once for MIMO TIBWB-OFDM, the received signal at the r^{th} receive antenna $Y_k^{(r)}$ can be regarded as of a block-based SC-type [33] and for SC-FDE schemes, a nonlinear equaliser offers an excellent performance [1], the EGC and MRC will have a superior performance in comparison with the one reached in MIMO-OFDM schemes. In this way, the iterative receivers based on EGC and MRC concepts, which not require complex matrix inversions and, as so, enables a low computational complexity, can be employed in the MIMO TIBWB-OFDM transceiver, and even showing high interference levels in the first iterations, they are able to approach the MFB with the following ones [11].

When using iterative EGC or MRC equalisation methods, the N_T estimated signals $\tilde{\mathbf{X}}_k = [\tilde{X}_{k,(1)}, ..., \tilde{X}_{k,(N_T)}]^T$, at the l^{th} iteration, are given by,

$$\tilde{\mathbf{X}}_k^{(l)} = \mathbf{F}_k^{(l)T} \mathbf{Y}_k - \mathbf{B}_k^{(l)T} \hat{\mathbf{X}}_k^{(l-1)} \quad , \tag{5.2}$$

where the feedforward filter $\mathbf{F}_k^{(l)}$ and feedback filter $\mathbf{B}_k^{(l)}$ can be given by the matrices (4.13) and (4.14) and, whose expressions can be written by (4.23) and (4.21) for the EGC and MRC equalisers, respectively. In this case, after doing the channel equalisation, i.e. reducing the precursors of the channel impulse response, it is necessary a complete unformatting of each TIBWB-OFDM symbol that concerns the following steps:

- ZP Removal and serial-to-parallel conversion;
- Time-deinterleaving;
- Matched filtering (windowing);
- Disassembly of each BWB-OFDM symbols in the component OFDM based blocks;
- Performing the DFT of these time-domain OFDM blocks in order to obtain the estimated OFDM symbols $\tilde{\mathbf{S}}_{k,i,(t)} : \{k = 0, ..., N - 1\}$ with $i = 0, ..., N_s - 1$ and $t = 0, ..., N_T - 1$.

Note that if channel coding and bit interleaving is used all these N_T estimated symbol streams are reassembled again and treated as a whole, i.e as a vector of symbols as shown in Figure 5.6. Then, a "hard" or "soft" decision is taken on each estimated value $\tilde{S}_{k,i,(t)}$ generating the "hard" or "soft" symbols $\hat{S}_{k,i,(t)}$, with $i = 0, ..., N_s - 1$, $t = 0, ..., N_T - 1$ and $k = 1, ..., N - 1$.

Unlike of what happens after the channel equalisation, in the feedback loop, a formatting of each one of the N_T TIBWB-OFDM blocks is needed, following the same procedure as the original data at the transmitter

side, composed by:

- Spatial Multiplexing and serial-to-parallel conversion;
- Cyclic extension and windowing;
- Time-interleaving and frame assembly, obtaining the N_T estimated blocks $\hat{\mathbf{x}}_{n,(t)}$ with $t = 0, ..., N_T - 1$.

Finally, the resulting estimates are converted back to the frequency domain by the means of a N_x-sized FFT, yielding the "hard" or "soft" decision $\hat{\mathbf{X}}_k = [\tilde{X}_{k,(1)}, ..., \tilde{X}_{k,(N_T)}]^T$. Both iterative methods (MRC and EGC) proceeds until the last iteration is performed.

On the other hand, when employing the MMSE or ZF equaliser, the receiver scheme is represented by the Figure 5.6, that consequently does not have a feedback loop, differing in only this aspect when compared with the iterative receiver presented in the Figure 5.5.

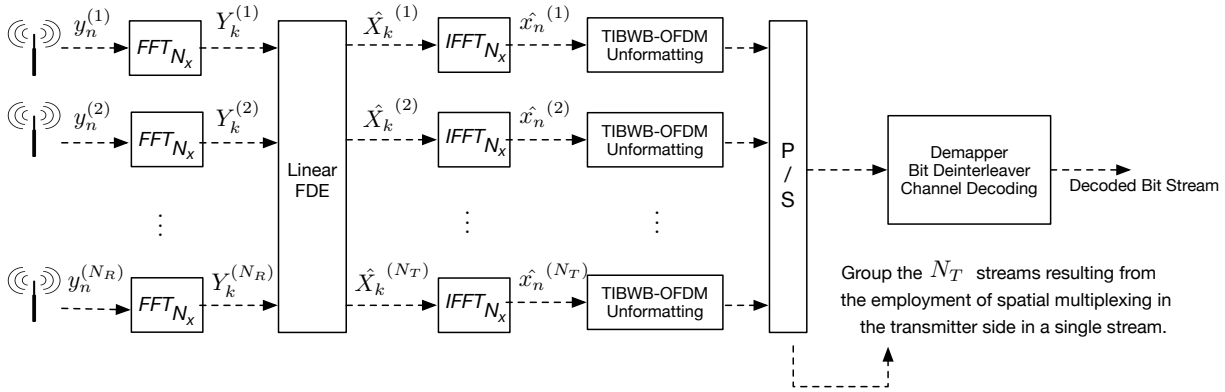

Figure 5.6: Forward Path of MIMO TIBWB-OFDM iterative corresponding to the Linear Frequency Domain Equalisation.

5.2.1 LLR Computation for Soft Decoding

The use of channel coding and soft-decoding techniques at reception can provide significant performance gains. However, these are highly dependent on the correct estimation of the log-likelihood ratio (LLR) of the received information. Common to both discussed receivers is the procedure taken on each symbol $\tilde{S}_{k,i,(t)}$, in order to achieve the "hard" or "soft" symbols. When attaining "soft" decisions and for QPSK constellations, the LLRs are given by,

$$\Lambda(b_0) = log\left(\frac{P_r(b_0 = 0|\hat{S}_{k,j,(t)}\,[m]}{P_r(b_0 = 1|\hat{S}_{k,j,(t)}\,[m]}\right) = \frac{4Re\left[\hat{S}_{k,j,(t)}\,[m]\right]}{\sigma_N^2} \quad . \tag{5.3}$$

$$\Lambda(b_1) = log\left(\frac{P_r(b_1 = 0|\hat{S}_{k,j,(t)}\,[m]}{P_r(b_1 = 1|\hat{S}_{k,j,(t)}\,[m]}\right) = \frac{4Im\left[\hat{S}_{k,j,(t)}\,[m]\right]}{\sigma_N^2} \quad . \tag{5.4}$$

For the MIMO scenario it is necessary to correctly estimate the noise variance σ_N^2. In this thesis we use two approaches proposed in [28] and [7], respectively, and by performing the necessary adaptations the estimate

of the noise variance can be given by,

$$\sigma_N^2 \approx \frac{\varepsilon_s}{N_x} \sum_{k=0}^{N_x-1} \frac{1}{1+SNR|H_k|^2} \quad , \tag{5.5}$$

with ε_s the variance of the original modulated symbols and $N_x = N_s \times N(1+\beta) + N_{ZP}$ for the MMSE receiver and,

$$\sigma_N^2 \approx \frac{1}{4NN_sN_T} \sum_{i=0}^{N_s-1} \sum_{k=0}^{N-1} \sum_{t=0}^{N_T-1} |\hat{S}_{k,i,(t)}^{(l)} - \tilde{S}_{k,i,(t)}^{(l)}|^2 \quad , \tag{5.6}$$

with $\tilde{S}_{k,i,(t)}$ being the estimated symbols and $\hat{S}_{k,i,(t)}$ being the "hard" decision taken on each $\tilde{S}_{k,i,(t)}$ for ZF and both iterative EGC and MRC receivers.

Finally, to estimate the original binary sequence, it is applied the original bit-deinterleaving and channel decoding. The obtained performance results using the concepts mentioned in this thesis proved to be quite consistent, being presented in the next chapter.

6 Performance Results

In this section, BER performance for the MIMO-OFDM and MIMO TIBWB-OFDM schemes for the SU-MIMO case employing the several receivers described in chapter 4 is presented. The user is assumed to have N_T antennas and the BS is equipped with N_R antennas. Three different scenarios will be discussed:

- Scenario A : With 4 transmit antennas and 4 receive antennas ($N_T = 4$ and $N_R = 4$). Since the proposed equalisation techniques are valid for $N_R \geq N_T$, this scenario represents the the worst case condition and, therefore, the associated BER performances will be, in general, very poor. Furthermore, for scenarios with $N_R < N_T$, the mathematical expressions of both iterative MRC and EGC are not valid.

- Scenario B : With 4 transmit antennas and 10 receive antennas ($N_T = 4$ and $N_R = 10$). This scenario represents an intermediate case with moderate values of N_R and N_T.

- Scenario C : With 4 transmit antennas and 16 receive antennas ($N_T = 4$ and $N_R = 16$). This scenario, that enables an increased N_R/N_T ratio, it is the most advantageous, allowing, in general, a substantial BER performance improvement.

These three scenarios consider a transmission over a severe time-dispersive channel with 32 symbol-spaced multipath components with uncorrelated Rayleigh fading. It is assumed perfect synchronisation, as well as, channel estimation at the receiver.

The BER results are shown considering the variation of E_b/N_0, with E_b denoting the average bit energy for the set of N_R receiving antennas (i.e. N_R times the bit energy for a single antenna) and N_0 denotes the unilateral power spectral density of the AWGN channel noise. The MFB is presented as a lower bound for the BER performance that can be reached.

6.1 MIMO-OFDM

The following simulations of the different scenarios consider OFDM transmission with $N = 64$ sub-carriers employing QPSK modulation under a Gray coding rule on each carrier. When using channel coding, it is employed a (128,64) short low-density parity-check (LDPC) code, and bit-interleaving is applied over thirty-two consecutive coded words. The conventional MIMO-OFDM is evaluated considering a CP with length $N_{CP} = N/4$, i.e. 25% of the OFDM symbol duration.

6.1.1 SISO CP-OFDM versus MIMO CP-OFDM

Figure 6.1 presents some BER results for the MIMO CP-OFDM scheme employing MMSE and ZF equalisers, and comparing them with SISO CP-OFDM scheme.

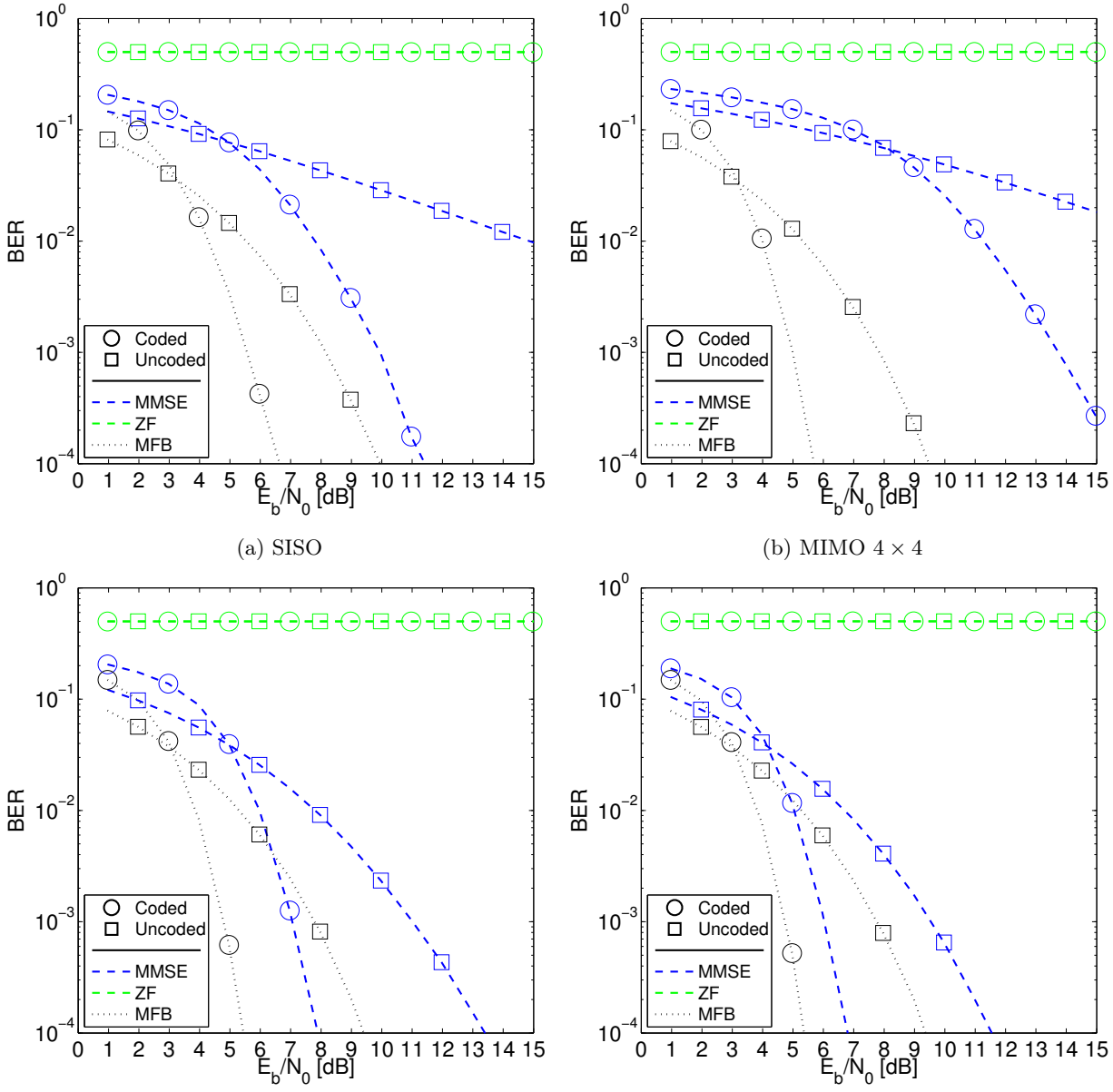

(a) SISO

(b) MIMO 4×4

(c) MIMO 4×10

(d) MIMO 4×16

Figure 6.1: BER results for MIMO CP-OFDM employing MMSE and ZF receivers for the scenario A,B and C, for both coded and uncoded transmissions, over a severe time-dispersive channel.

In comparison to the SISO case, it seems that the MIMO case in the scenario A (MIMO 4×4) does not outperform the SISO case. However, these MIMO BER figures considers the overall transmitted power of the system, making the MIMO gain not noticed in comparison with SISO. Therefore, there is in fact a gain over the SISO gain. Whether these figures had been presented as function of the power per receive antenna, the MIMO performance would have been superior over the SISO gain, making noticeable the effective gain provided by MIMO. In fact, and picking the example of the scenario A (MIMO 4×4), if there are four transmit antennas sending a data stream each one, this receive antenna will receive the sent stream per transmit antenna and, therefore, the associated power grow four times, having a gain much more higher

than in SISO.

When considering the scenarios B (MIMO 4×10) and C (MIMO 4×16), the MIMO case employing the MMSE equaliser demonstrates a significant performance improvement, achieving gains of about 3.7dB and 4.7dB, respectively, over the SISO scheme, when channel coding used. In fact, the advantage of MMSE over ZF is that it does not amplify too much the noise in the presence of deep fading, being able to cancel the ISI and interference between transmitted streams in a more efficient way.

Finally, it is possible to verify that the increase in the number of receiving antennas allows to improve considerably the performance of the overall system.

6.1.2 MIMO-OFDM under EGC and MRC iterative equalisation

This section presents the BER results for the MIMO CP-OFDM scheme employing MMSE and both iterative EGC and MRC equalisers.

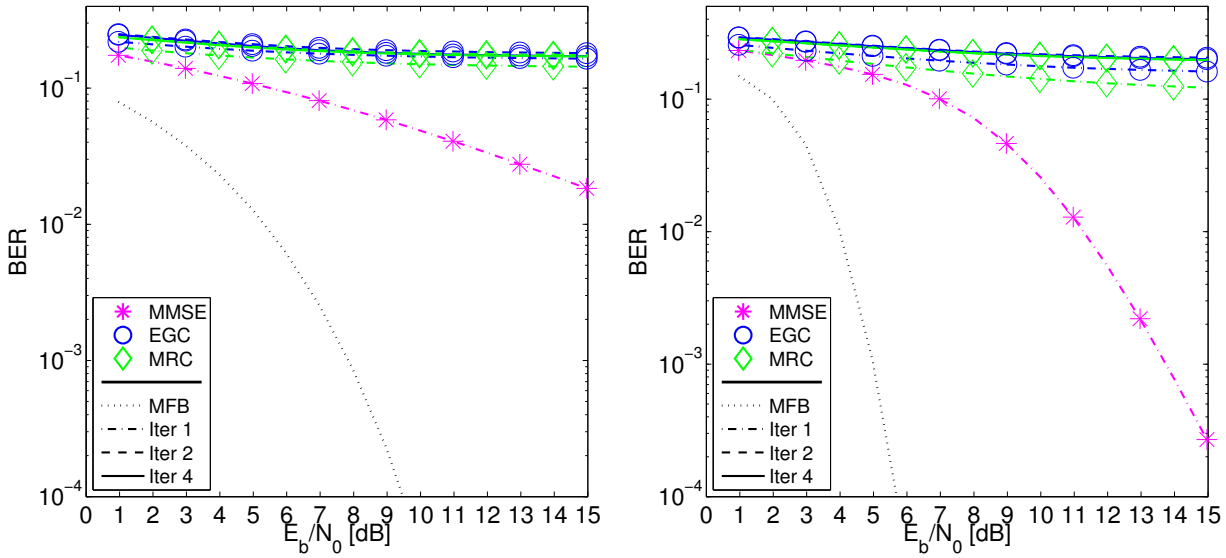

(a) Uncoded Transmission MIMO 4×4

(b) Coded Transmission MIMO 4×4

Figure 6.2: BER results for MIMO CP-OFDM employing MMSE and both iterative EGC and MRC receivers for the scenario A, for both coded and uncoded transmissions, over a severe time-dispersive channel.

Firstly, as previously mentioned, since the MRC and EGC equalisers are only applicable to scenarios with $N_R \geq N_T$, Figure 6.2 presents the performance of this equalisers for the worst case scenario, i.e. for the scenario A (MIMO 4×4). As expected, the performance of these receivers is unsatisfactory, even in the 4^{th} iteration of each method. Actually, the poor cancellation at the first iteration of the ISI effect and interference between different transmitted streams, that are too high, causes an error floor for both coded and uncoded transmissions. In fact, the ability of iterative equalisers to converge, depends on a reasonable degree of cancellation of ISI and interference between streams at the first iteration. In this case, the MMSE receiver has clearly the best BER performance due to the trade-off between noise enhancement and ISI mitigation that is achieved through this type of receiver.

In comparison with the scenario A (MIMO 4×4), the considered equalisers in the scenarios B (MIMO 4×10) and C (MIMO 4×16) can achieve a significant improvement on their BER performances for higher

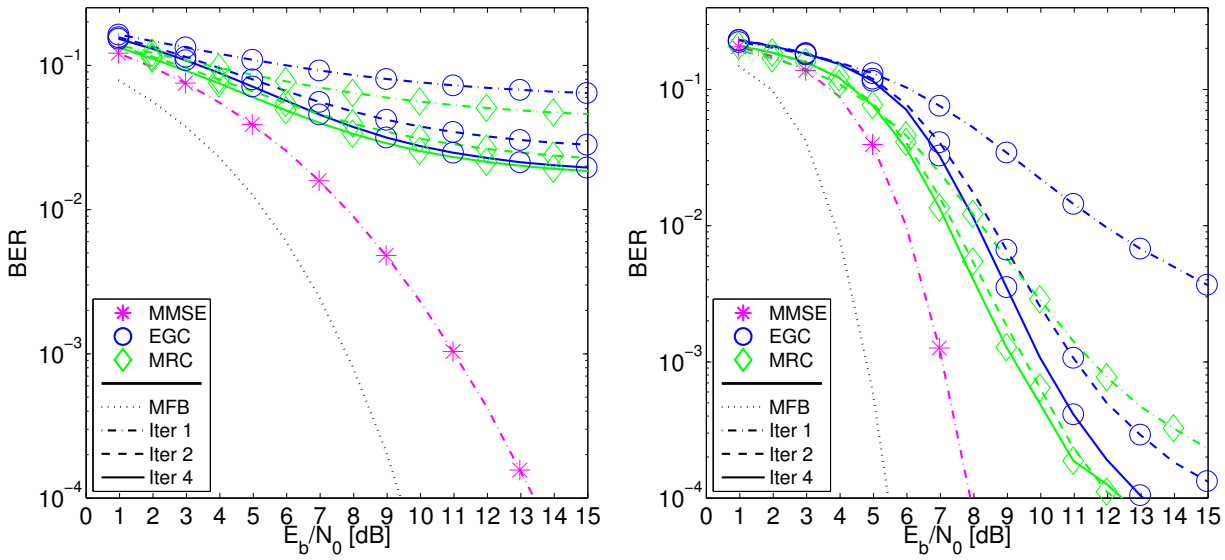

(a) Uncoded Transmission MIMO 4×10 (b) Coded Transmission MIMO 4×10

Figure 6.3: BER results for MIMO CP-OFDM employing MMSE and both iterative EGC and MRC receivers for the scenario B, for both coded and uncoded transmissions, over a severe time-dispersive channel.

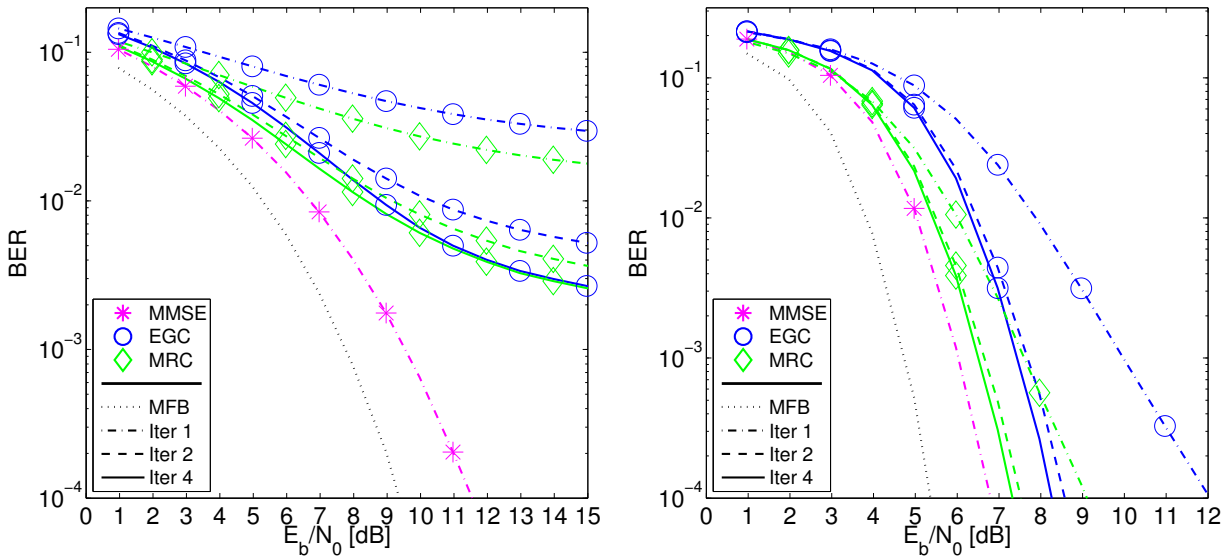

(a) Uncoded Transmission MIMO 4×16 (b) Coded Transmission MIMO 4×16

Figure 6.4: BER results for MIMO CP-OFDM employing MMSE and both iterative EGC and MRC receivers for the scenario C, for both coded and uncoded transmissions, over a severe time-dispersive channel.

values of N_R (receive antennas) as shown in Figures 6.3 and 6.4. Particularly, both EGC and MRC at the 4^{th} iteration can reach a considerable enhancement on their performances, although the 1^{st} iteration of each equaliser, which corresponds to the simple EGC and MRC method, produces worse results. In this way, for both scenarios, the successive iteration can improve the BER performance, being these receivers able to minimise the residual interference levels and efficiently separate the received data streams, while taking advantage of the signal contributions associated with a given transmit antenna at each receive antenna of the BS, especially for MRC. The MMSE receiver still outperforms once again both EGC and MRC receivers by 5dB and 4.5dB for the scenario B (MIMO 4×10) and by 2dB and 0.6dB for the scenario C (MIMO 4×16), respectively, when channel coding is used. However, it is clear that the interferences (ISI and the

interference between different transmitted streams) can be reduced with an increase in N_R/N_T ratio, being the scenario C (MIMO 4×16) mentioned as the best case scenario.

Even though MMSE presents in all the cases a better performance, we can approach it with an equaliser conceived with much lower complexity as long as the number of receiving antennas is high, making the iterative MRC and EGC equalisers as a good solution for massive MIMO applications, where matrix inversion imposed by MMSE can be problematic. Actually for the scenario C (MIMO 4×16), the MRC can approach the MMSE performance, setting itself apart from the MFB by about 2dB after four iterations.

6.2 MIMO TIBWB-OFDM

The following simulations of the different scenarios consider $N = 64$ sub-carriers, and QPSK modulation under a Gray coding rule. Also, both consider that each transmit antenna sends a TIBWB-OFDM symbol of length $N_x = 4096$ formed by $N_s = 42$ OFDM based blocks and employing a SRRC window with $\beta = 0.5$. When using channel coding, it is used a (128,64) short LDPC code, and bit-interleaving is applied over 42 consecutive coded words, i.e. per single megablock associated to the different transmit antennas. Its performance is compared with the conventional MIMO-OFDM that is evaluated considering a CP with length $N_{CP} = N/4$, i.e. 25% of the OFDM symbol duration.

6.2.1 MIMO CP-OFDM versus MIMO TIBWB-OFDM

Figure 6.5 presents the BER results for the MIMO CP-OFDM and MIMO TIBWB-OFDM scheme, employing MMSE and ZF equalisers.

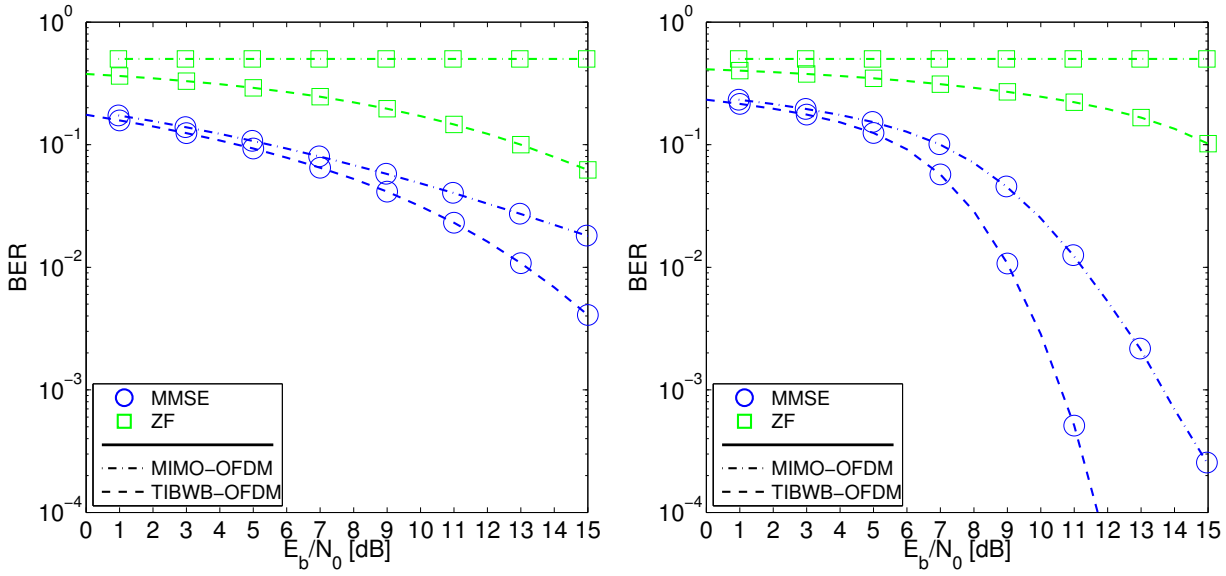

(a) Uncoded Transmission MIMO 4×4

(b) Coded Transmission MIMO 4×4

Figure 6.5: BER results for MIMO CP-OFDM and MIMO TIBWB-OFDM employing MMSE and ZF receivers for the scenario A, for both coded and uncoded transmissions, over a severe time-dispersive channel.

For all the scenarios, the BER performance of the MIMO TIBWB-OFDM scheme is superior in comparison with the one verified in MIMO CP-OFDM, for both coded and uncoded transmission, being something already expected since the first mentioned technique not only enables to replicate de data information

throughout the bandwidth and therefore preserve all data susceptible of being destroyed, but also a higher both spectral and power efficiency.

When comparing the performance of ZF and MMSE for MIMO TIBWB-OFDM, we can observe that the MMSE equaliser outperforms the case in which ZF equaliser is used, owing to its trade-off between noise enhancement and ISI mitigation.

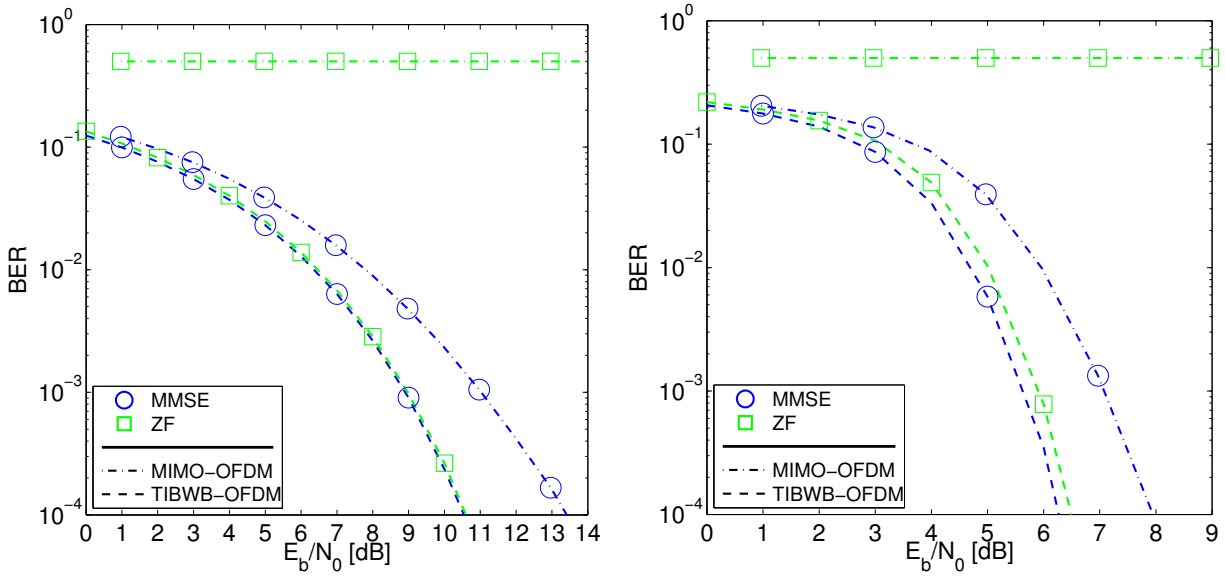

(a) Uncoded Transmission MIMO 4×10 (b) Coded Transmission MIMO 4×10

Figure 6.6: BER results for MIMO CP-OFDM employing MMSE and ZF receivers for the scenario B, for both coded and uncoded transmissions, over a severe time-dispersive channel.

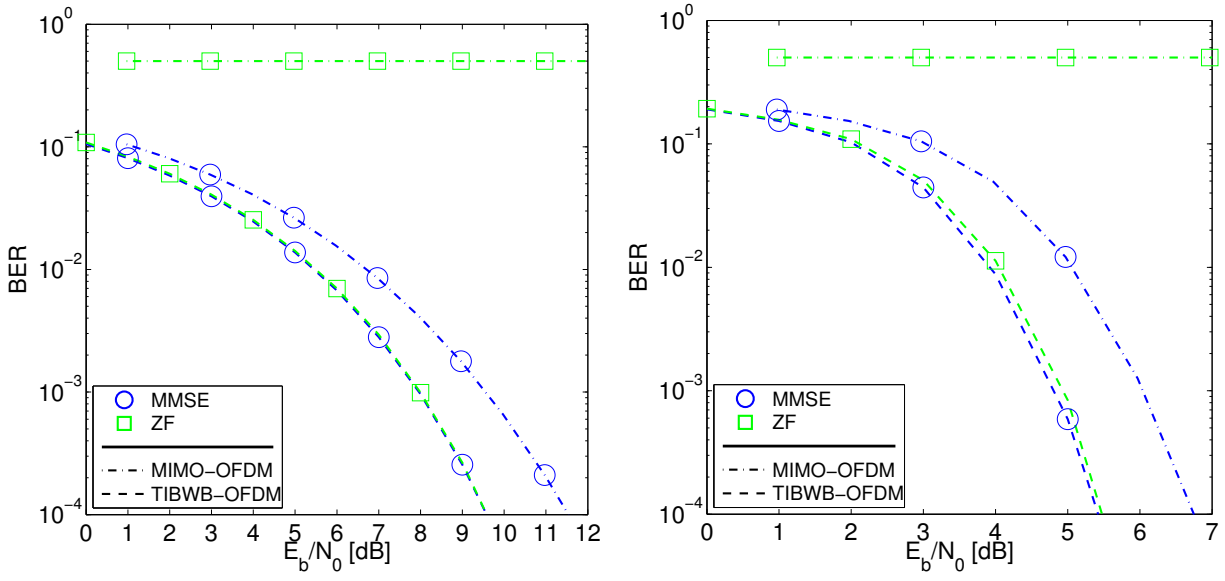

(a) Uncoded Transmission MIMO 4×16 (b) Coded Transmission MIMO 4×16

Figure 6.7: BER results for MIMO CP-OFDM employing MMSE and ZF receivers for the scenario C, for both coded and uncoded transmissions, over a severe time-dispersive channel.

However this is not the case when the number of receiving antennas is increased. Figures 6.6 and 6.7 show the performance for scenarios B (MIMO 4×10) and C (MIMO 4×16). The increase in the number of receiving antennas combined with the characteristic of the MIMO TIBWB-OFDM scheme, which lies on

the possibility of having spare data containing the original information in the several subcarriers, dilutes the effect of possible catastrophic deep fading occurrences due to the several degrees of diversity. In addition, in these scenarios the ZF equaliser can easily replace the MMSE, yielding a much more simpler system.

6.2.2 MIMO TIBWB-OFDM under EGC and MRC iterative equalisation

Figure 6.8, 6.9 and 6.10 presents the BER performance of the MIMO TIBWB-OFDM scheme employing the MMSE, EGC and MRC equalisers, for the scenarios A (MIMO 4×4), B (MIMO 4×10) and C (MIMO 4×16), respectively.

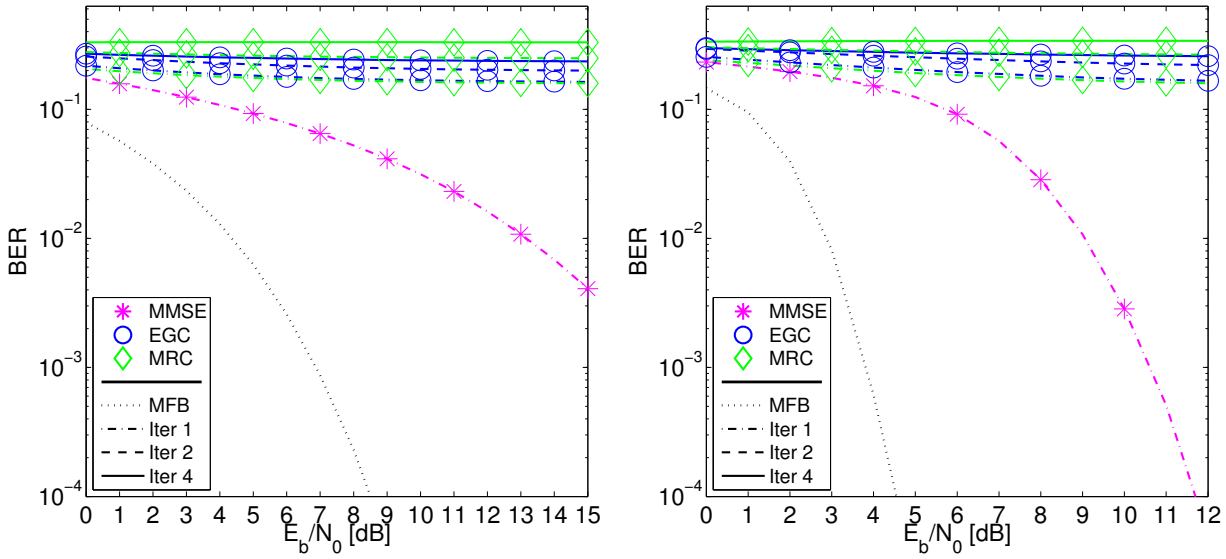

(a) Uncoded Transmission MIMO 4×4

(b) Coded Transmission MIMO 4×4

Figure 6.8: BER results for MIMO TIBWB-OFDM employing MMSE and iterative EGC and MRC receivers for the scenario A, for both coded and uncoded transmissions, over a severe time-dispersive channel.

Similar to MIMO CP-OFDM, the scenario A (MIMO 4×4) is the worst case scenario, since as previously mentioned the mathematical expressions of the iterative receivers EGC and MRC are only valid for cases with $N_R \geq N_T$. For this reason, their performances are, in general, very poor, being not able to minimise the high residual interference levels (both ISI and interference between the transmitted streams) so efficiently.

For scenario B (MIMO 4×10), both EGC and MRC receivers at the 4^{th} iteration can achieve a significant enhancement on their BER performances, being able to approach the MMSE receiver. For scenario C (MIMO 4×16), these receivers can achieve an excellent performance, being highlighted the MRC method, approaching the MFB by only less than 0.5dB after just 4 iterations. Thus, both iterative iterative equalisers MRC and EGC can converge to an unitary matrix after a few iterations, decreasing the correlation level between the different received signals and as so being clear that the residual interferences can be reduced with an increase in N_R/N_T ratio.

Finally, note the excellent BER performances of the iterative receivers for uncoded transmissions, which in particular for the scenario C (MIMO 4×16) the MRC can approach the MFB after 4 iterations.

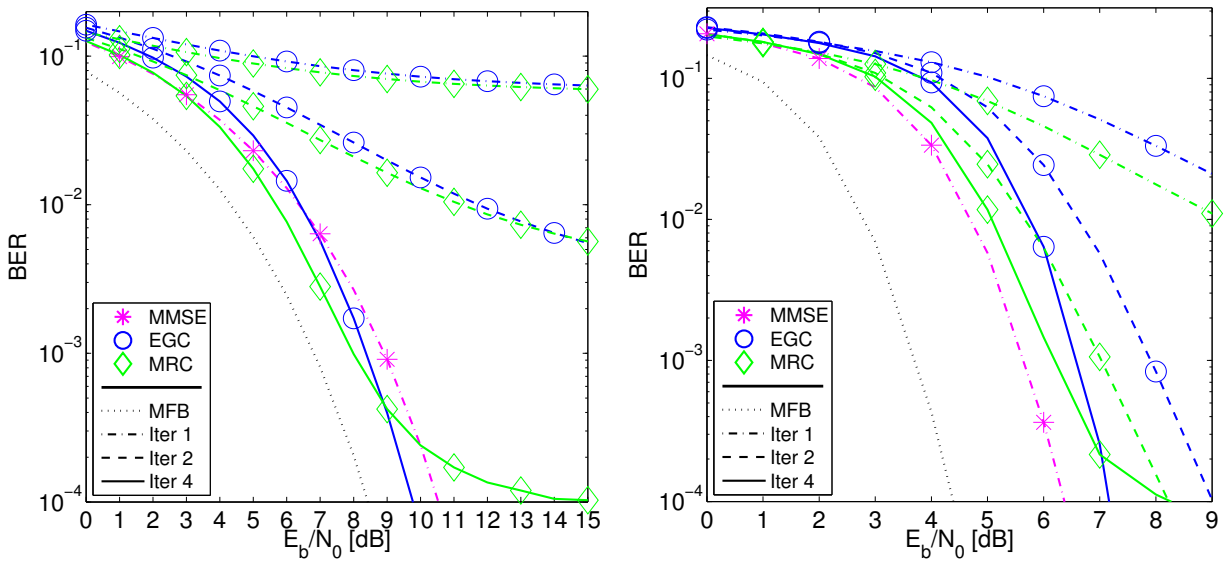

(a) Uncoded Transmission MIMO 4×10

(b) Coded Transmission MIMO 4×10

Figure 6.9: BER results for MIMO TIBWB-OFDM employing MMSE and iterative EGC and MRC receivers for the scenario B, for both coded and uncoded transmissions, over a severe time-dispersive channel.

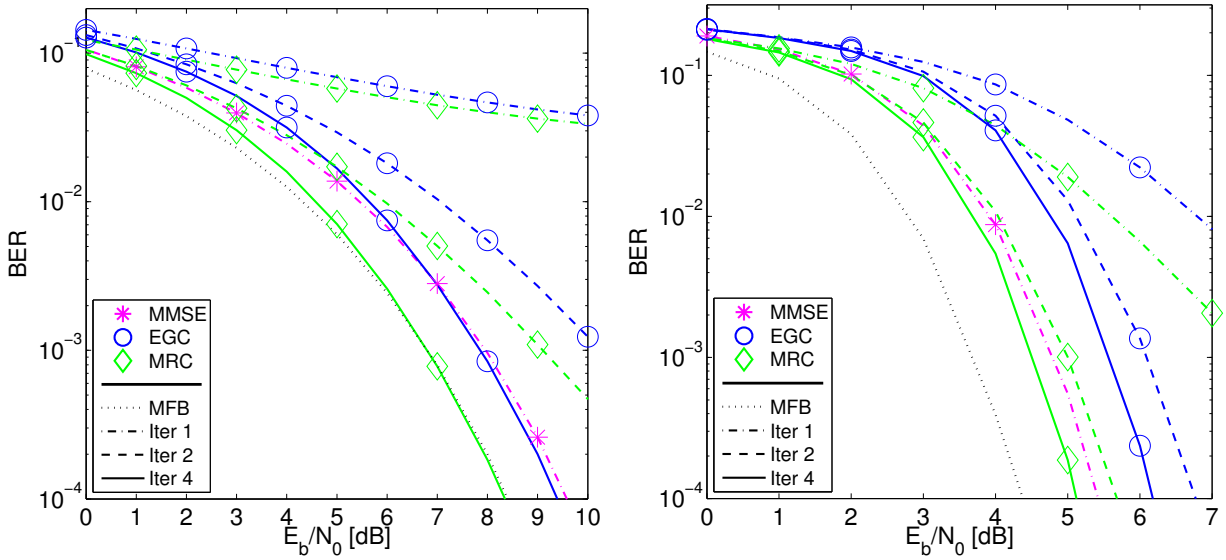

(a) Uncoded Transmission MIMO 4×16

(b) Coded Transmission MIMO 4×16

Figure 6.10: BER results for MIMO TIBWB-OFDM employing MMSE and iterative EGC and MRC receivers for the scenario C, for both coded and uncoded transmissions, over a severe time-dispersive channel.

6.2.3 MIMO BWB-OFDM versus MIMO TIBWB-OFDM

In this section, it is compared the performance of TIBWB-OFDM and BWB-OFDM under a MIMO transmission. Firstly, remember that the TIBWB-OFDM transceiver (see Figure 5.4 and 5.5) only differs in one aspect when compared with BWB-OFDM (see Figure 2.4 and 2.6), the employment of the time-interleaving procedure, that is performed at no complexity cost.

The obtained results, presented in the Figure 6.11, proves that when MIMO is combined with the TIBWB-OFDM scheme, it continues having a better BER performance than combined with BWB-OFDM, for both uncoded and coded transmissions like in the SISO case (see Figure 2.10), showing once again the improvement inherent to the time-interleaver approach, that save up most part of the corrupted data thought

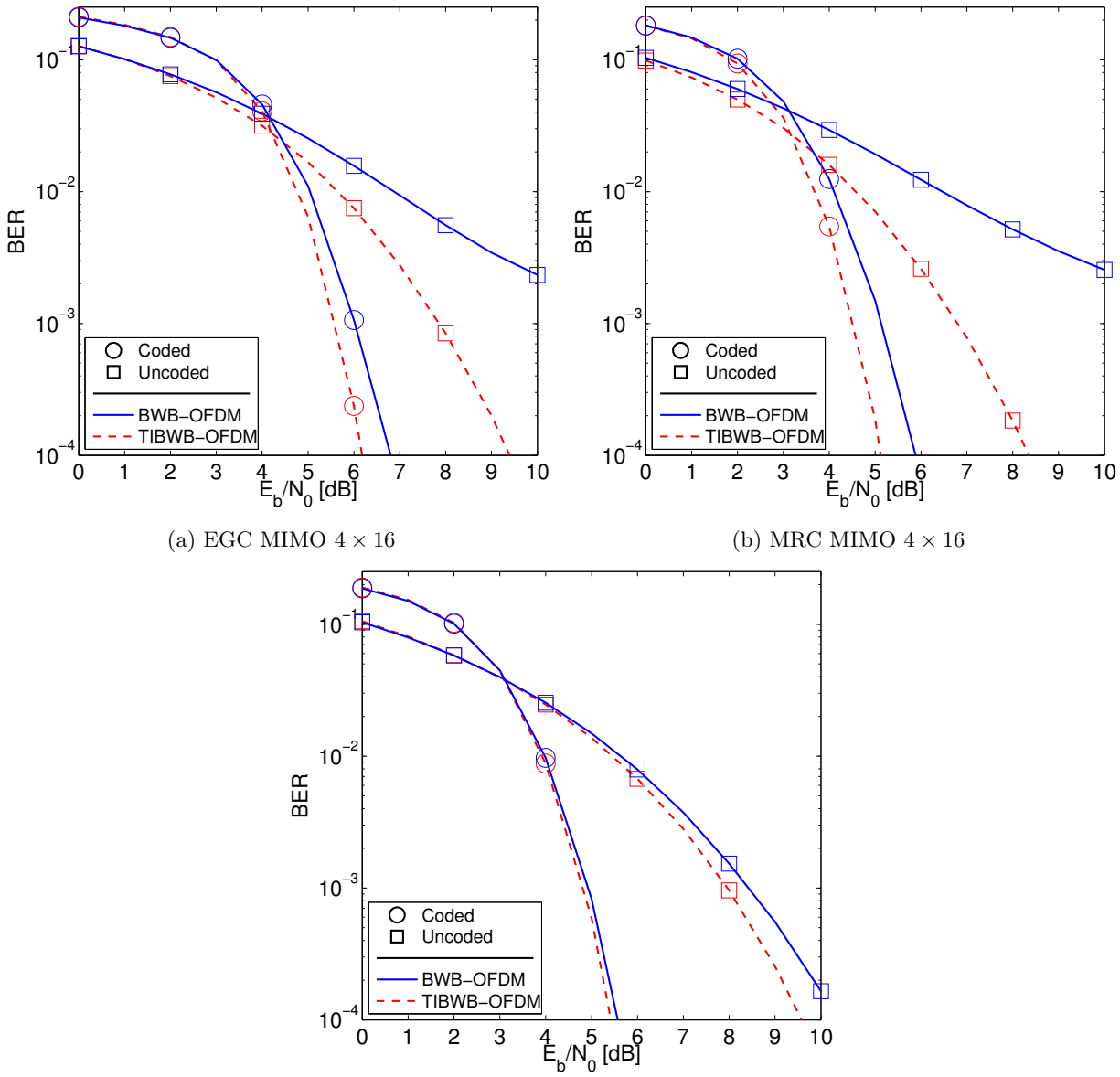

(a) EGC MIMO 4×16

(b) MRC MIMO 4×16

(c) MMSE MIMO 4×16

Figure 6.11: BER results for MIMO BWB-OFDM and MIMO TIBWB-OFDM employing MMSE and iterative EGC and MRC receivers for the scenario C considering both uncoded and coded transmission, over a severe time-dispersive channel.

multiple replicas of the transmitted data. Consider a MIMO 4×16 scenario, for a coded transmission, the gain of MIMO TIBWB-OFDM scheme over the MIMO BWB-OFDM is about 0.8dB, 1dB and 0.1dB employing EGC, MRC and MMSE, respectively.

When employing a MMSE equaliser, the MIMO BWB-OFDM performance is really close to the one of the MIMO TIBWB-OFDM, meaning that the spatial diversity associated to the channel in an advantageous scenario of $N_R \gg N_T$ (that is being considered) can dilute the diversity effect offered by the TIBWB-OFDM technique, not being relevant to the success of the system in this particular case. On the other hand, for the remaining considered scenarios, this diversity effect has an important role in order to achieve favorable performances.

6.2.4 Final Remarks

Firstly, MIMO TIBWB-OFDM scheme can reach better performances than MIMO CP-OFDM, particularly for the low complexity iterative equalisers, not only due to the MIMO TIBWB-OFDM scheme characteristics, such as higher spectral and power efficiency and robustness against the deep fades of the channel, but also because this nonlinear equalisers allow to achieve superior performances in SC-FDE schemes [1] (remember that at reception TIBWB-OFDM block can be seen as of SC-FDE type signal).

In the scenario B (MIMO 4×10) and when considering a coded transmission, although MMSE receiver still outperforms both EGC and MRC iterative receivers, they can approach its performance in a much more simpler way, reducing the complexity inherent to inversion matrix verified in MMSE. When comparing the iterative EGC and MRC receivers, EGC has the best performance, being more interesting for intermediate situations, i.e. scenarios with moderate values of N_R and N_T.

In scenario C (MIMO 4×16), MRC have the best performance when compared with the EGC and MMSE, being therefore considered as a promising iterative frequency domain receiver for this specific situation. This receiver does not require channel matrix inversions as well and as expected, when the N_R/N_T relation increases, the received SNR also increases, being possible to achieve an enhanced performance.

In this way, both iterative EGC and MRC represent promising methods to decrease the overall system's complexity. Note that it is crucial to cancel the high residual interference levels presented in their first iterations, namely the ISI and interference between transmitted data streams, being useful to have iterative receivers able to completely mitigate this interferences in the following iterations. The MRC receiver is not the best choice to case scenarios with smaller values of N_R and N_T, as it enhances the ISI effect. On the other hand, since in EGC method the ISI effect is not worsened, this receiver offers good performances for the previous mentioned scenarios.

7 Conclusions

A huge growth in data traffic is to be expected in the next decade, sending part of the research efforts for the development of the fifth generation of wireless networks. This will have to incorporate a wide range of solutions capable of fulfilling capacity demands. One possible and extremely promising alternative consists in the employment of multiple antennas at both transmitter as receiver, meaning a substantial increase in spectral efficiency, which must be achieved while maintaining or even improving the power efficiency. However, there is an additional complexity associated to these type of systems, exhibiting high dimension channel matrices, that become unbearable mainly in massive MIMO.

The focus of this thesis was turned to MIMO-OFDM type systems able to achieve both spectral and power efficiency and to deal with the frequency-selective MIMO channel, while keeping the receiver complexity reduced through the use of techniques that does not require channel matrix inversions. For this purpose, a MIMO system based on TIBWB-OFDM scheme and employing low complexity iterative EGC and MRC receivers was conceived in order to met all the requirements previously mentioned. Since this scheme represents an improved version of MIMO BWB-OFDM and, consequently, of MIMO CP-OFDM, it shows significant gains for any considered scenario and receiver. If on one hand in the MIMO-OFDM case, the low complexity iterative EGC and MRC receivers can approach but never outperforms the linear MMSE receiver, in the MIMO TIBWB-OFDM they can approach as well or even outperform the linear receiver. Specifically, for a MIMO scenario 4×16 with MRC receiver a considerable BER performance can be reached only about 0.5dB from the MFB, being the scenario where it is easier to separate the received signals in a more efficient way, i.e. the interferences (ISI and interference between the different transmitted streams) can be easily reduced, and therefore it is considered the best case scenario.

Aiming attention to the iterative frequency domain EGC and MRC receivers, when a MIMO TIBWB-OFDM scheme is assumed, the obtained BER performances showed that EGC represents a good alternative to scenarios with moderate number of antennas. On the other hand, MRC can approach the MFB by about 0.5dB being an excellent receiver for cases with an increased N_R/N_T ratio.

On the whole, it was demonstrated in this thesis that the complexity inherent to the MIMO systems can be successfully surpassed using the low complexity iterative EGC and MRC receivers, attaining excellent performances particularly when they are employed in a MIMO TIBWB-OFDM scheme.

7.1 Future Work

This dissertation presented analysis and alternative solutions to overcome the computational complexity inherent to MIMO systems, especially useful for massive MIMO, being possible to achieve a highly spectral

and power efficient system. Although the obtained results, mostly for MIMO TIBWB-OFDM, were quite satisfactory, there are some several interesting directions for future work:

- Testbed implementation of the MIMO TIBWB-OFDM scheme employing both low complexity iterative EGC and MRC receivers.
- Implementation of a MU-MIMO system combined with the several techniques approached in this dissertation: the proposed SU-MIMO takes advantage of the correlation between the transmitted data streams. More specifically, since the MIMO signal received is a linear combination of the multiple data streams, interference between the transmitted streams arises. However, this type of interference is cancelled by the equalisers described in the section 4.2. Furthermore, since the original data stream is coded and interleaved as a whole, the data stream estimated that is deinterleaved and decoded will also be treated as a whole. In fact, this estimated data stream is the reassembling of the N_T data streams when the SM technique is applied. Thus, the N_T data streams are correlated with each other. In this way, the receiver takes advantage of this correlation that is used by the deinterleaver and decoder in order to correct all the erroneous bits, and hence, reach the original data stream. For this reason, it would be very interesting to compare MU-MIMO with SU-MIMO, since in the first one the data streams are from different users and consequently independents from each other.
- Design of the IB-DFE receiver in a MIMO environment: the proposed receiver requires channel matrix inversions and, as so, its complexity increases with the number of antennas elements. In this way, a comparison of these receivers with the iterative EGC and MRC equalisers would be essential to fully validate their performances.
- Employment of the SD MIMO technique and/or a combination of it with SM (already developed in this dissertation) in order to compare both techniques and/or maybe to achieve a commitment between these two.

8 Bibliography

[1] *Intersymbol Interference in Digital Communication Systems*. Wiley Online Library, 2001.

[2] P. Bento, A. Pereira, R. Dinis, M. Gomes, and V. Silva. Low complexity receivers for mmwave massive mimo systems with sc-fde modulations. 2016.

[3] N. Benvenuto, R. Dinis, D. Falconer, and S. Tomasin. Single carrier modulation with nonlinear frequency domain equalization: An idea whose time has come-again. *Proceedings of the IEEE*, 98(1):69–96, Jan 2010.

[4] Ezio Biglieri, Robert Calderbank, Anthony Constantinides, Andrea Goldsmith, Arogyaswami Paulraj, and H. Vincent Poor. *MIMO Wireless Communications*. Cambridge University Press, New York, NY, USA, 2007.

[5] D. W. Bliss, A. M. Chan, and N. B. Chang. Mimo wireless communication channel phenomenology. *IEEE Transactions on Antennas and Propagation*, 52(8):2073–2082, Aug 2004.

[6] D. Borges, P. Montezuma, and R. Dinis. Low complexity mrc and egc based receivers for sc-fde modulations with massive mimo schemes. Washington DC, USA, Dec 2016. IEEE GLOBALSIP'2016.

[7] F. Cercas, F. Ribeiro, R. Dinis, and A. Silva. Uplink of base station cooperation systems with sc-fde modulations and ib-dfe receivers. In *Conf. on Telecommunications - ConfTele*, volume WL1.1, pages 1–5, May 2013.

[8] X. Cheng, Y. He, B. Ge, and C. He. A filtered ofdm using fir filter based on window function method. In *2016 IEEE 83rd Vehicular Technology Conference (VTC Spring)*, pages 1–5, May 2016.

[9] Tzi-Dar Chiueh and Pei-Yun Tsai. *OFDM Baseband Receiver Design for Wireless Communications*. Wiley Publishing, 2007.

[10] Yong Soo Cho, Jaekwon Kim, Won Young Yang, and Chung G. Kang. *MIMO-OFDM Wireless Communications with MATLAB*. Wiley Publishing, 2010.

[11] F. Coelho, R. Dinis, N. Souto, and P. Montezuma. On the impact of multipath propagation and diversity in performance of iterative block decision feedback equalizers. In *2010 IEEE 6th International Conference on Wireless and Mobile Computing, Networking and Communications*, pages 246–251, Oct 2010.

[12] Nelson Costa and Simon Haykin. *Multiple-input, multiple-output channel models : theory and practice*. Wiley series in adaptive and learning systems for signal processing, communication and control. IEEE, Institute of Electrical and Electronic Engineers Hoboken, N.J. John Wiley, New York, 2010.

[13] S. N. DIGGAVI, N. AL-DHAHIR, A. STAMOULIS, and A. R. CALDERBANK. Great expectations: the value of spatial diversity in wireless networks. *Proceedings of the IEEE*, 92(2):219–270, Feb 2004.

[14] R. Dinis and P. Montezuma. Iterative receiver based on the egc for massive mimo schemes using sc-fde modulations. *Electronics Letters*, 52(11):972–974, 2016.

[15] K.L. Du and M.N.S. Swamy. *Wireless Communication Systems: From RF Subsystems to 4G Enabling Technologies*. Cambridge University Press, 2010.

[16] R. Calderbank et al. E. Biglieri. *MIMO Wireless Communications*. Cambridge University Press, New York, NY, USA, 2007.

[17] B. Farhang-Boroujeny. Ofdm versus filter bank multicarrier. *IEEE Signal Processing Magazine*, 28(3):92–112, May 2011.

[18] W. Fisher. *Digital Video and Audio Broadcasting Technology: A Practical Engineering Guide*. Springer, 2008.

[19] G.J. Foschini and M.J. Gans. On limits of wireless communications in a fading environment when using multiple antennas. *Wireless Personal Communications*, 6(3):311–335, March 1998.

[20] D. Gesbert, M. Kountouris, R. W. Heath Jr., C. b. Chae, and T. Salzer. Shifting the mimo paradigm. *IEEE Signal Processing Magazine*, 24(5):36–46, Sept 2007.

[21] D. Gesbert, M. Shafi, Da shan Shiu, P. J. Smith, and A. Naguib. From theory to practice: an overview of mimo space-time coded wireless systems. *IEEE Journal on Selected Areas in Communications*, 21(3):281–302, Apr 2003.

[22] Andrea Goldsmith. *Wireless Communications*. Cambridge University Press, New York, NY, USA, 2005.

[23] E. S. Gopi. *Digital Signal Processing for Wireless Communication Using Matlab*. Springer Publishing Company, Incorporated, 1st edition, 2015.

[24] Uma Shanker Jha and Ramjee Prasad. *OFDM Towards Fixed and Mobile Broadband Wireless Access*. Artech House, Inc., Norwood, MA, USA, 2007.

[25] M. Jiang and L. Hanzo. Multiuser mimo-ofdm for next-generation wireless systems. *Proceedings of the IEEE*, 95(7):1430–1469, July 2007.

[26] J.Nunes. Sistema ofdm multi-símbolo: Uma abordagem multiportadora eficiente. Master's thesis, University of Coimbra, 2014.

[27] Ui-Kun Kwon, Gi-Hong Im, and Jong-Bu Lim. Mimo spatial multiplexing technique with transmit diversity. *IEEE Signal Processing Letters*, 16(7):620–623, July 2009.

[28] Yuan-Pei Lin, See-May Phoong, and P. P. Vaidyanathan. *Filter Bank Transceivers for OFDM and DMT Systems*. Cambridge University Press, New York, NY, USA, 2010.

[29] A. Lozano and N. Jindal. Transmit diversity vs. spatial multiplexing in modern mimo systems. *IEEE Transactions on Wireless Communications*, 9(1):186–197, January 2010.

[30] B. Muquet, Zhengdao Wang, G. B. Giannakis, M. de Courville, and P. Duhamel. Cyclic prefixing or zero padding for wireless multicarrier transmissions? *IEEE Transactions on Communications*, 50(12):2136–2148, Dec 2002.

[31] Richard van Nee and Ramjee Prasad. *OFDM for Wireless Multimedia Communications*. Artech House, Inc., Norwood, MA, USA, 1st edition, 2000.

[32] H. Quoc Ngo. Massive mimo: Fundamentals and system designs. Master's thesis, Linköping University, 2015.

[33] J. Nunes, P. Bento, M. Gomes, R. Dinis, and V. Silva. Block-windowed burst ofdm: a high-efficiency multicarrier technique. *Electronics Letters*, 50(23):1757–1759, 2014.

[34] Arogyaswami Paulraj, Rohit Nabar, and Dhananjay Gore. *Introduction to Space-Time Wireless Communications*. Cambridge University Press, New York, NY, USA, 1st edition, 2008.

[35] R. Penrose. On the reciprocal of the general algebraic matrix. *Proceedings of the Cambridge Philosophical Society*, 51:406–413, 1955.

[36] Jyrki TJ Penttinen. *The Telecommunications Handbook: Engineering Guidelines for Fixed, Mobile and Satellite Systems*. John Wiley & Sons, 2015.

[37] Y. Rahmatallah and S. Mohan. Peak-to-average power ratio reduction in ofdm systems: A survey and taxonomy. *IEEE Communications Surveys Tutorials*, 15(4):1567–1592, Fourth 2013.

[38] T. G. Simões, M. Gomes, V. Silva, and R. Dinis. Time-interleaved block-windowed burst ofdm. In *IEEE Vehicular Technology Conf. - VTC-Fall*, volume -, pages —, September 2016.

[39] G. L. Stuber, J. R. Barry, S. W. McLaughlin, Ye Li, M. A. Ingram, and T. G. Pratt. Broadband mimo-ofdm wireless communications. *Proceedings of the IEEE*, 92(2):271–294, Feb 2004.

[40] I. Emre Telatar. Capacity of multi-antenna gaussian channels. *European Transactions on Telecommunications*, 10(6):585–595, Dec 1999.

[41] T.Fernandes. Time-interleaved bwb-ofdm with iterative fde. Master's thesis, University of Coimbra, 2015.

[42] L. Yu, B. D. Rao, L. B. Milstein, and J. G. Proakis. Reducing out-of-band radiation of ofdm-based cognitive radios. In *Signal Processing Advances in Wireless Communications (SPAWC), 2010 IEEE Eleventh International Workshop on*, pages 1–5, June 2010.

[43] Lizhong Zheng and David N. C. Tse. Diversity and multiplexing: a fundamental tradeoff in multiple-antenna channels, 2003.

[44] Zhouhua, Yangdacheng, Qiweishi, and MaMin. On performance of mutiuser diversity in siso and mimo wireless communication. In *Personal, Indoor and Mobile Radio Communications, 2003. PIMRC 2003. 14th IEEE Proceedings on*, volume 3, pages 2872–2875 vol.3, Sept 2003.